Mineralogical Magazine (2024), **88**, 111–126
doi:10.1180/mgm.2023.87

CAMBRIDGE UNIVERSITY PRESS

Article

Mn–Fe-rich genthelvite from pegmatites associated with the Madeira Sn–Nb–Ta deposit, Pitinga, Brazil: new constraints on the magmatic-hydrothermal transition in the albite-enriched granite system

Ingrid W. Hadlich[1], Artur C. Bastos Neto[1], Vitor P. Pereira[1], Nilson F. Botelho[2], Luiz H. Ronchi[3] and Harold G. Dill[4]

[1]Instituto de Geociências, Universidade Federal do Rio Grande do Sul, Av. Bento Gonçalves 9500, 91501-970 Porto Alegre, RS, Brazil; [2]Instituto de Geociências, Universidade de Brasília, Campus Universitário Darcy Ribeiro, Asa Norte, 70910-900 Brasília, DF, Brazil; [3]Centro de Engenharias, Universidade Federal de Pelotas, Praça Domingos Rodrigues 2, 96010-440 Pelotas, RS, Brazil; and [4]Gottfried Wilhelm Leibniz University, Welfengarten 1, D-30167 Hannover, Germany

Abstract

Genthelvite from pegmatite veins hosted by the albite-enriched granite (ca.1.8 Ga) corresponding to the Sn–Nb–Ta (F, REE, Li, Zr, U, Th) Madeira deposit, Amazonas, Brazil was studied. Genthelvite, the exclusive Be-bearing mineral within the deposit, occurs as massive crystals of up to 4.7 cm in size. Compositions are homogeneous within individual crystals, although there is moderate variation in the overall composition reflecting relatively limited substitutions within the helvine–genthelvite–danalite solid-solution series, with relatively high Zn contents (36.96 to 49.45 wt.% ZnO), lower Mn contents (0.61 to 3.03 wt.% MnO), and variable Fe contents (2.10 to 10.94 wt.% FeO), completing an existing compositional gap in this system. Genthelvite formed in an alkaline and subaluminous environment, under stable conditions within the late-evolved fluids, at relatively high temperature (>400°C), in a reducing environment. The extremely high concentration of fluorine in the magma and the crystallisation of magmatic galena resulted in an effective reduction of H_2S fugacity. This resulted in the stabilisation of genthelvite during the transition from the late magmatic to early hydrothermal stages of the albite-enriched granite evolution. The variability in Fe content within genthelvite is associated primarily with localised variations in the mineral assemblage (e.g. the presence of riebeckite and polylithionite). Genthelvite was altered by low-temperature aqueous fluids rich in F which resulted in the incorporation of Fe, Mn, Mg, Pb, Ba, Na, K, U and REE into the Zn^{2+} structural site and the allocation of excess Si, Al, Ti and P in the ^{IV}Si and ^{IV}Be structural sites. The substantial content of U and REE substituting for Zn, together with Si substituting for Be, is charge balanced by the presence of vacancies at the A site.

Keywords: genthelvite; beryllium; solid solution; albite-enriched granite; Pitinga; Brazil

(Received 16 April 2023; accepted 3 November 2023; Accepted Manuscript published online: 13 February 2024; Associate Editor: František Laufek)

Introduction

Helvine-group minerals are anhydrous sulfosilicates, cubic and isostructural with the space group $P\bar{4}3n$ and are sodalite structural types. They have the general formula $A_8Be_6(SiO_4)_6S_2$, in which the species are defined by the cation in the A crystallographic site. The species helvine ($Mn_4Be_3Si_3O_{12}S$), danalite ($Fe_4Be_3Si_3O_{12}S$) and genthelvite ($Zn_4Be_3Si_3O_{12}S$) form a solid solution, whose proportions are defined by the states of reduction, sulfidation and alkalinity of the system (Burt, 1980). Complete miscibility should exist between the three end-members (Hassan and Grundy, 1985), however, compositional gaps exist between the end-members Zn–Fe, Zn–Mn and Mn–Fe and pure danalite has not been observed in Nature (Oftedal and Saebø, 1963; Clark and Fejer, 1976; Dunn, 1976; Larsen, 1988; Perez *et al.*, 1990; Langhof *et al.*, 2000; Bilal, 2013).

The helvine-group minerals are only found in peralkaline and alkaline granites, syenites, rare metal pegmatites, albitites, greisens, skarns and contact zones (Deer *et al.*, 2004). In this work, we have investigated the occurrence of genthelvite in pegmatite veins hosted by the albite-enriched granite facies of the Madeira granite. This facies corresponds to the Madeira deposit, which is characterised by an association of Sn with cryolite, Nb, Ta, Y, rare earth elements (REE), Li, Zr, U and Th in the same albite-enriched granite that hosts a massive cryolite deposit. The genthelvite crystals occur in pegmatite veins found in the most differentiated portion in the centre of the pluton. These pegmatites fit in the CMS (Dill, 2016) classification as the 24dE type because they are hosted in peralkaline igneous rocks and are carriers of REE–Y ores. According to the classification in Černý and Ercit (2005), they belong to the Rare Elements class and the NYF family, as they are rich in REE, Nb, Y and F, and are associated

Corresponding author: Ingrid W. Hadlich; Email: ingrid.hadlich@ufrgs.br
Cite this article: Hadlich I.W., Bastos Neto A.C., Pereira V.P., Botelho N.F., Ronchi L.H. and Dill H.G. (2024) Mn–Fe-rich genthelvite from pegmatites associated with the Madeira Sn–Nb–Ta deposit, Pitinga, Brazil: new constraints on the magmatic-hydrothermal transition in the albite-enriched granite system. *Mineralogical Magazine* **88**, 111–126. https://doi.org/10.1180/mgm.2023.87

with A-type granites in environments with low pressures and temperatures. The study of genthelvite brings new constraints on the conditions of the magmatic-hydrothermal transition in the albite-enriched granite system.

Previous work

Geological setting

The Pitinga Province is located (Fig. 1) in the southern portion of the Guyana Shield (Almeida *et al.*, 1981), in the Tapajos-Parima Tectonic Province (Santos *et al.*, 2000). The volcanic rocks of the Iricoume Group (Veiga *et al.*, 1979) predominate in the Pitinga Province (Fig. 1) and have $^{207}Pb/^{206}Pb$ zircon ages between 1881 ± 2 and 1890 ± 2 Ma (Ferron *et al.*, 2006). They consist mostly of effusive and hypabyssal rhyolites, highly welded ignimbrites, ignimbritic tuffs, and surge deposits formed in a subaerial environment with cyclic effusive and explosive activities (Pierosan *et al.*, 2011; Simões *et al.*, 2014). The Iricoume Group host the Madeira Granite (Fig. 1).

The Madeira granite (Figs 1, 2) contains four facies (Horbe *et al.*, 1991; Lenharo *et al.*, 2003; Costi *et al.*, 2005, 2009; Bastos Neto *et al.*, 2009). The oldest, mostly metaluminous porphyritic amphibole–biotite granite (1824 ± 2 Ma, Costi *et al.*, 2000), contains plagioclase-mantled K-feldspar megacrysts, sometimes have reverse-zoned K-feldspar-mantled plagioclase ovoids, and is usually referred to as the 'rapakivi' subfacies. The amphibole–-biotite granite was followed by the metaluminous biotite granite (1822 ± 2 Ma, Costi *et al.*, 2000). The younger facies are the hypersolvus porphyritic alkali feldspar granite (1818 ± 2 Ma, Costi *et al.*, 2000) and the albite-enriched granite (Fig. 2). The latter is the host to the pegmatites investigated in this work. The age of the albite-enriched granite is only very roughly constrained at 1822 ± 22 Ma (Bastos Neto *et al.*, 2014) due to the metasomatic alteration of zircons. According to Costi (2000), these younger facies were emplaced simultaneously. The hypersolvus granite has K-feldspar phenocrysts in a fine- to medium-grained matrix composed dominantly of K-feldspar and quartz.

The albite-enriched granite

The albite-enriched granite is an oval-shaped body with a surface outcrop of ~2×1.3 km. It is divided into subfacies of a core albite-enriched granite and a border albite-enriched granite. The core albite-enriched granite is a peralkaline subsolvus granite, porphyriticto-seriate in texture, fine-to-medium grained, and composed of quartz, albite and K-feldspar in approximately equal proportions (25–30%). The accessory minerals are cryolite (5%), polylithionite (4%), green–brown mica (3%), zircon (2%) and riebeckite (2%). Pyrochlore, cassiterite, xenotime, columbite, thorite, magnetite and galena occur in minor proportions. The border albite-enriched granite is peraluminous and exhibits types of texture and essential mineralogy similar to that of the core albite-enriched granite, except for being richer in zircon, with fluorite instead of cryolite. Iron-rich silicate minerals are absent, having been completely removed by autometasomatic processes (Costi *et al.*, 2000, 2009).

The Madeira rare-metal deposit

The Pitinga Province is the largest Sn producer in Brazil. The alluvial ore deposits were discovered in 1979 (Veiga *et al.*, 1979) and are almost exhausted. The primary ores are associated mainly with the Madeira deposit, which has been exploited since 1989. The Madeira deposit corresponds to the albite-enriched granite facies of the Madeira Granite and presents disseminated ore with

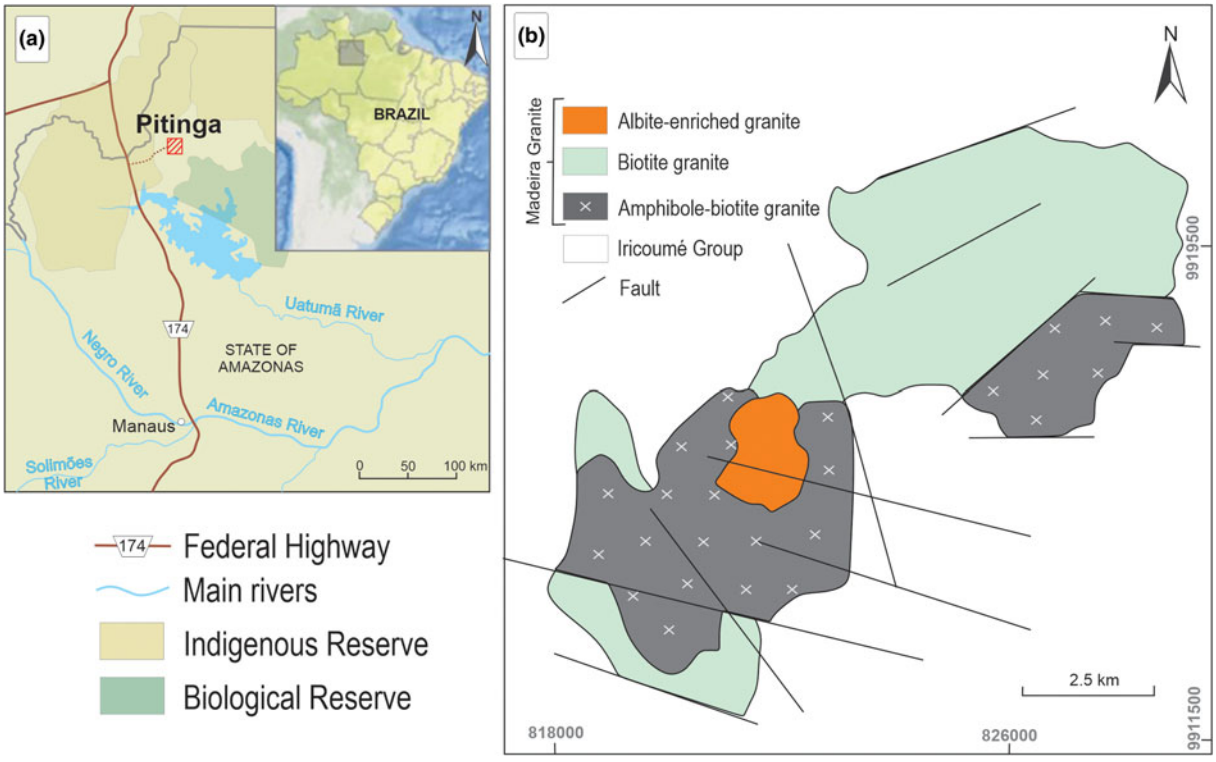

Figure 1. (a) Location map and (b) geological map of the Madeira Granite, Pitinga, Brazil (modified from Costi, 2000).

https://doi.org/10.1180/mgm.2023.87 Published online by Cambridge University Press

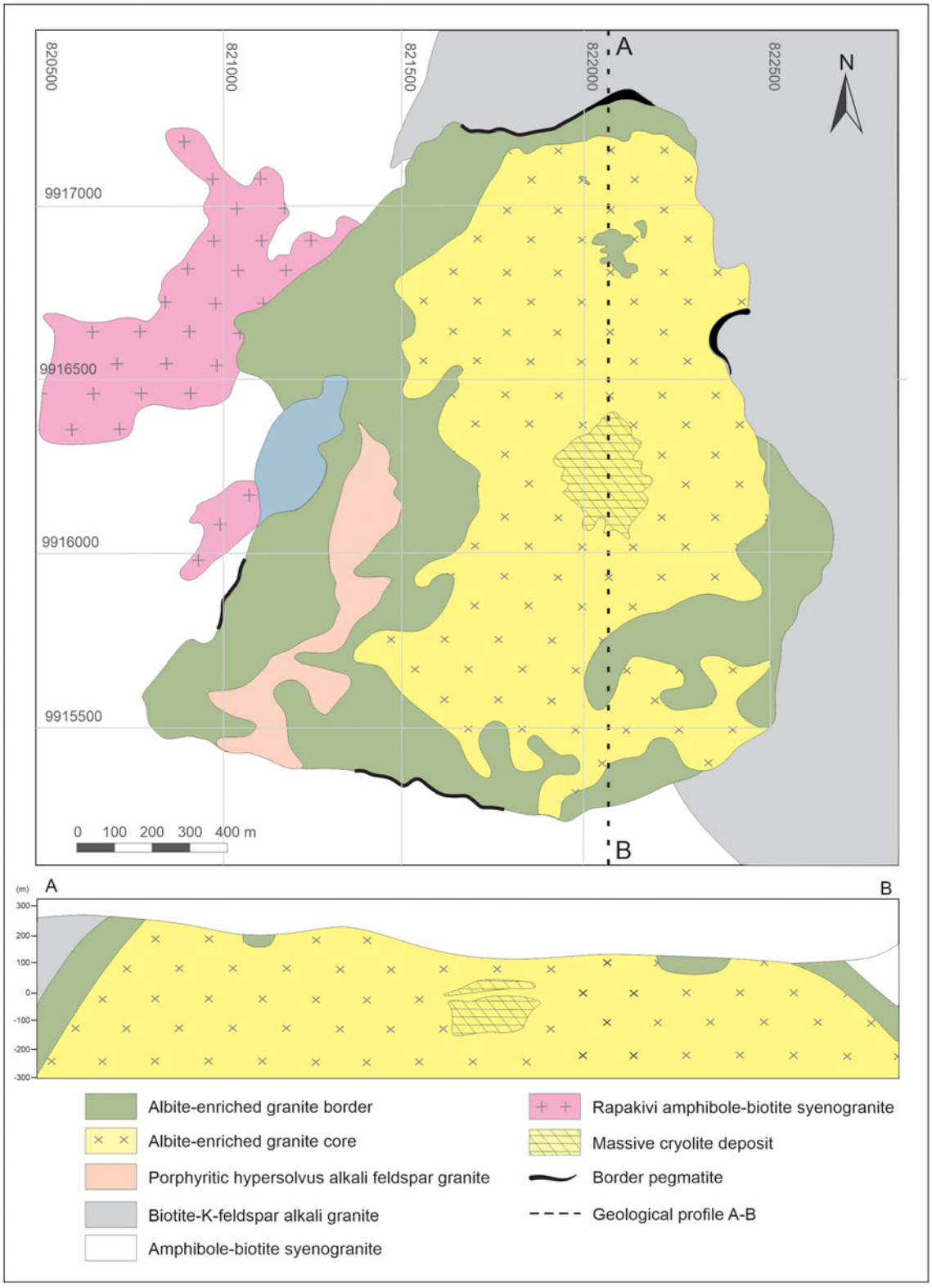

Figure 2. Geological map of the albite-enriched granite (modified from Minuzzi, 2005).

grades of 0.17 wt.% Sn (cassiterite), 0.20 wt.% Nb_2O_5) and 0.024 wt.% Ta_2O_5 (both in pyrochlore and columbite). The potential by-products of the disseminated ore are F (4.2 wt.% cryolite), Y and heavy rare earth elements (HREE) (xenotime), Zr and Hf (zircon), Th (0.07 wt.% ThO_2, thorite), and U (pyrochlore). Regardless of the disseminated character of the albite-enriched granite mineralisation, there are small zones of enrichment associated with the granite in which particular minerals are considerably abundant. These are: (1) thick pods and bands of the pegmatitic albite-enriched granite (~50 cm, rarely up to 10 m thick; Stolnik,

https://doi.org/10.1180/mgm.2023.87 Published online by Cambridge University Press

2015) that show gradational contacts with the albite-enriched granite; These contain the same minerals as the core albite-enriched granite, although polylithionite, riebeckite, xenotime and thorite are more abundant and of large size; (2) border pegmatites at the contact between the border albite-enriched granite and the older facies (Fig. 2) characterised by increased size and amounts of quartz and zircon, advanced alterations of K-feldspar and biotite and by local enrichments in fluorite, polylithionite, thorite and secondary hematite (Lengler, 2016); (3) several bodies of massive cryolite intercalated with core albite-enriched granite and hypersolvus granite, which are sub-horizontal, up to 300 m long and 30 m thick and composed of cryolite (~87 vol.%), quartz, zircon and feldspar (Minuzzi *et al.*, 2006); and (4) pegmatite veins (Paludo *et al.*, 2018; Ronchi *et al.*, 2019) which are not mappable, occur more commonly in the central, northern and northwest parts of the core albite-enriched granite, and have thicknesses ranging from a few centimetres up to 2 m. Genthelvite occurs only in these pegmatite veins and was first identified by Ronchi *et al.* (2011). There are two types of pegmatite veins visible in the whole mine front (140 to 210 meters above sea level) hosted by the core albite-enriched granite. The prevalent type is that of tabular bodies emplaced in horizontal extension fractures. The other group is formed by tabular bodies emplaced in subvertical reverse fault planes. These fractures and faults served as a conduit for the fluids, with transportation from southwest to northeast, in a compressive system, with horizontal tension and at low solidus temperature (Ronchi *et al.*, 2019). These have been separated into three groups in Paludo *et al.* (2018) on the basis of composition and modal values as: (1) those rich in amphibole (riebeckite, fluoro-arfvedsonite and fluoro-eckermannite), with intermediate contents of K and Na; (2) rich in polylithionite, with high K contents; and (3) cryolite-rich, with high Na contents.

Evolution of the albite-enriched granite system

Bastos Neto *et al.* (2009, 2014) consider that the A-type magmatism in Pitinga evolved in a post-collisional extensional setting, probably in a within-plate scenario in which extensional and trans-tensional tectonic regimes dominated. In this context, the albite-enriched granite magma would have been related to the isotherm rise, which occurred when the mantle fluid ascended further into the crust promoting fenitisation-type reactions (Martin, 2006) in rocks previously enriched in Sn, and introduced elements such as F, Nb, Y, REE and Th in anomalous concentrations. The input of a F-rich fluid generated metasomatism causing the rock to become fusible.

Lenharo (1998) and Costi (2000) considered that the albite-enriched granite magma evolved towards an extremely Na-, F-enriched residual melt. Costi (2000) interpreted that, at the point of H_2O saturation, the extremely F-enriched residual fluid separated into an aqueous, relatively F-poor portion and a low-H_2O, Na–Al–F-rich portion. The latter fraction resulted in the formation of massive cryolite bodies, whereas the H_2O-rich fraction formed the associated quartz-, feldspar- and mica-bearing pegmatitic rocks. In accordance with Bastos Neto *et al.* (2009), extreme fluorine enrichment in the residual melt is unlikely to have been attained because the F content was buffered by crystallisation of magmatic cryolite (Dolejs and Baker, 2007). Furthermore, fluid-inclusion data (Bastos Neto *et al.*, 2009; Ronchi *et al.*, 2011) show that the massive cryolite deposit was formed from an aqueous, saline hydrothermal fluid. The higher homogenisation temperature of 400°C, measured in massive cryolite, determines the minimum starting temperature for the hydrothermal process.

Methods

Genthelvite crystals from several pegmatitic veins were described and identified by combining optical properties, using compositional analyses and powder X-ray diffraction data. The pegmatite veins are spread throughout the core albite-enriched granite and are not mappable due to their small size (up to 2 m thick). Sampling was carried out mainly in the central area of the core albite-enriched granite, on the surface of the open pit. Over 50 thin sections of the pegmatites were analysed and, among those which contained genthelvite, 10 were examined by back-scattered electron microscopy (BSE), with qualitative analysis using an energy-dispersive X-ray detector (Zeiss, model EVO MA10) at the Centre for Microscopy and Microanalysis in Universidade Federal do Rio Grande do Sul (UFRGS).

Mineral compositions of genthelvite were obtained using electron probe micro-analysis (EPMA) (JEOL JXA-8230) at the EPMA Laboratory of the Universidade de Brasília (UnB). The operation conditions were: 15 kV accelerating voltage and 10 nA beam current (F, Mg, Zn, Al, Si, Hf, Nb, P, Cl, S, Bi, Ti, Mn, Y, Ta, Sn, Ca, Zr, Fe, V and Rb), and 20 kV and 50 nA (Na, Er, Tm, Yb, Ho, Lu, K, Pb, Dy, Tb, Sm, Gd, Eu, Sr, Th, Pr, Nd, Ce, La, Ba and U), 1 μm beam diameter, and interference corrections were applied in all cases of peak overlap. The wavelength dispersive X-ray spectrometer (WDS) crystals used were: TAP (Si, Zn, Na, Al); PETJ (Nb, P, Hf, Cl, S, K, Bi, Sr, Y, Ta, Sn, Th, Pb); PETH (Rb, Zr, U); LIF (Ti, Mn, Sm, Eu, Gd, Dy, Er, Ho, Tb, Tm, Yb, Lu), LIFH (Ca, Fe, Ba, V, La, Ce, Pr, Nd); and LDE1 (F). The counting times on the peaks were 10 s for all elements, and half that time for background counts on both sides of the peaks. The following natural and synthetic standards were used: microcline (Si, K, Al); albite (Na); apatite (P; Ca); andradite (Fe); topaz (F); forsterite (Mg); vanadinite (V, Pb, Cl); pyrite (S); $MnTiO_3$ (Mn); YFe_2O_{12} (Y); $LiNbO_3$ (Nb); $LiTaO_3$ (Ta); $MnTiO_3$ (Ti, Mn); ZnS (Zn); Bi_2O_3 (Bi); RbSi (Rb); $BaSO_4$ (Ba); baddeleyite (Zr); PbS (Pb); HfO_2; $SrSO_4$ (Sr); SnO_2; ThO_2; UO_2; and synthetic REE-bearing glasses.

Crystallographic investigations were performed in the X-ray diffraction laboratory at UFRGS using a Siemens D5000 X-ray Diffractometer (XRD) with a scanning step of 0.05°2θ, a time of 1 s, between 5 and 100°2θ, Cu*K*α radiation (1.5418 Å) and a Ni filter. Crystallographic parameters were determined using the *UnitCell* program (Holland and Redfern, 1997), and the diffractions of 19 (reflections) faces were processed. The error in the processed values was 0.00017, with 95% reliability. The crystallographic information files have been deposited with the Principal Editor of *Mineralogical Magazine* and are available as Supplementary material (see below).

Results

Mineralogy and petrography

The contact of the pegmatite veins with the host rock is abrupt, marked by a thin, well-defined border, typically on the scale of centimetres. From the border towards the centre of the bodies, there is a systematic increase in the size of the minerals, though without the establishment of a clear zoning pattern. The interior of the bodies is homogeneous, characterised by anhedral to subhedral minerals. In most veins, the pegmatitic texture is marked

https://doi.org/10.1180/mgm.2023.87 Published online by Cambridge University Press

by crystals (up to 10 cm) of polylithionite, quartz, cryolite, microcline and albite, by crystals (up to 7 cm) of riebeckite, xenotime and genthelvite, and crystals (up to 3 cm) of thorite, galena and, more rarely, zircon, cassiterite and gagarinite.

Both the horizontal and the subvertical pegmatite veins exhibit the same mineralogical composition. The paragenetic succession is illustrated in Fig. 3. The major mineral assemblage consists of quartz, microcline, cryolite, polylithionite and riebeckite. The minor minerals are xenotime, thorite, gagarinite-(Y), and genthelvite. Accessory minerals are zircon, cassiterite, pyrochlore, columbite, galena, sphalerite, native lead, native bismuth, pyrite, hematite and chlorite. The matrix primarily consists of albite, quartz and grains are commonly anhedral, colourless in natural 0.3–1 cm. Additionally, polylithionite, cryolite and riebeckite are present. The entire magmatic paragenesis has undergone significant alteration due to the influence of F-rich hydrothermal fluids, ultimately leading to the formation of the secondary phases depicted in Fig. 3.

Genthelvite crystals from the pegmatite veins hosted by the core albite-enriched granite have sizes from 1.0 mm to 4.7 cm and present a light pink colour in macroscopic samples (Fig. 4). Optically, the grains are commonly anhedral, colourless in natural light and isotropic in polarised light (Fig. 5a,b). In the pegmatites genthelvite occurs predominantly as massive aggregates of crystals surrounding polylithionite and magmatic quartz and includes the accessory minerals pyrochlore, thorite and zircon (Fig. 5a–d). Subordinately, genthelvite occurs filling voids and microfractures in magmatic quartz (Fig. 5e) and polylithionite phenocrysts or arranged interstitially in the matrix with magmatic quartz and orthoclase (Fig. 5f).

The contact with polylithionite is rectilinear and slightly reactive. The contact with magmatic quartz is undulated and shows reactive rims. The contact with pyrochlore, zircon and thorite is undulated and reactive, and these minerals have a partially dissolved aspect. The samples show evidence of hydrothermal alteration. Genthelvite is characterised by corrosion features such as cavities and microfractures which are commonly filled by hydrothermal cryolite (Fig. 5g). Hydrothermal quartz also occurs associated with genthelvite, specifically filling the channels opened along genthelvite growth lines (Fig. 5h). On the basis of these

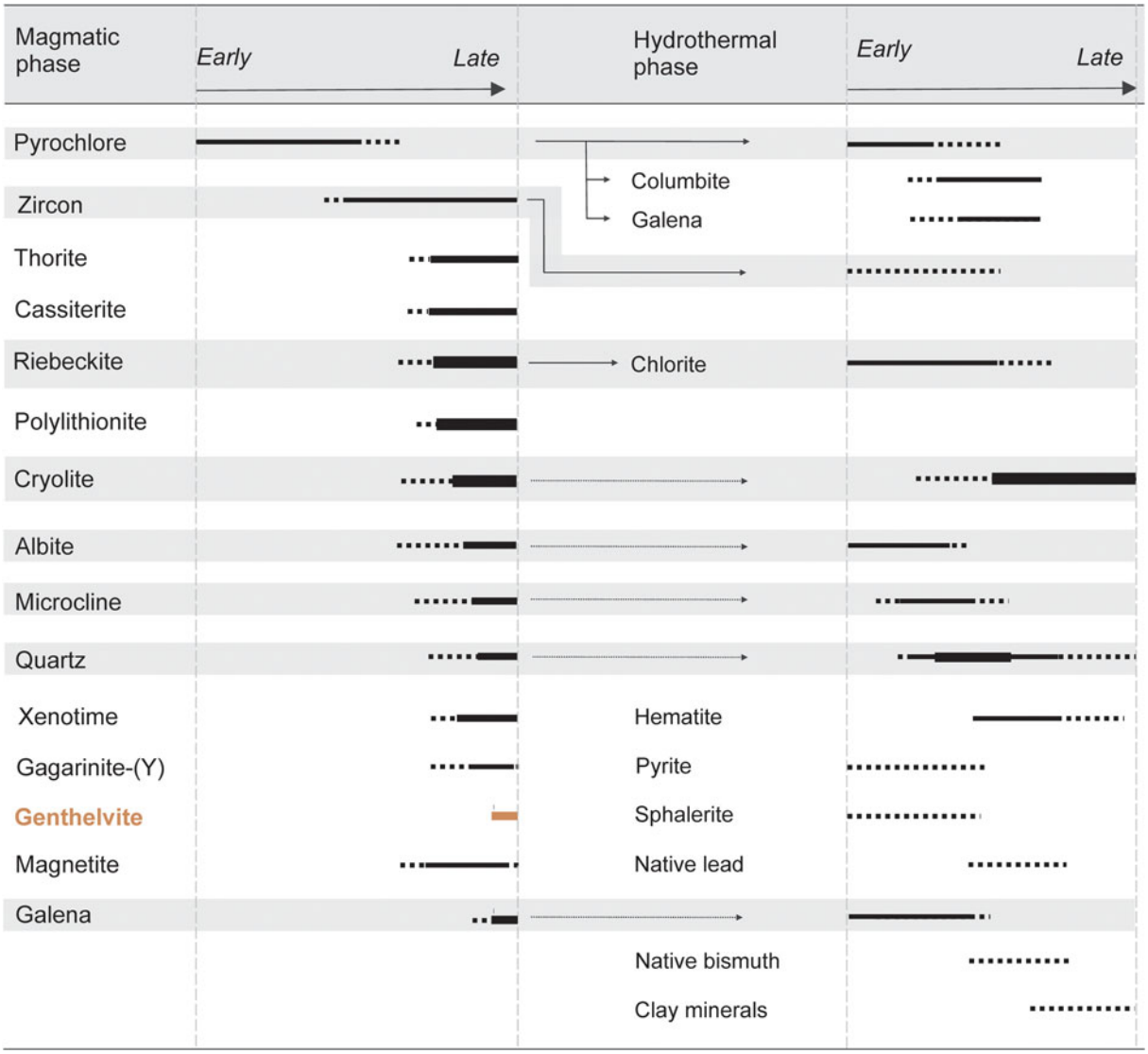

Figure 3. Paragenetic evolution of the genthelvite-bearing pegmatite veins. The line thickness is indicative of the abundance of the mineral. The precursor minerals for the most important replacement reactions are indicated by arrows.

https://doi.org/10.1180/mgm.2023.87 Published online by Cambridge University Press

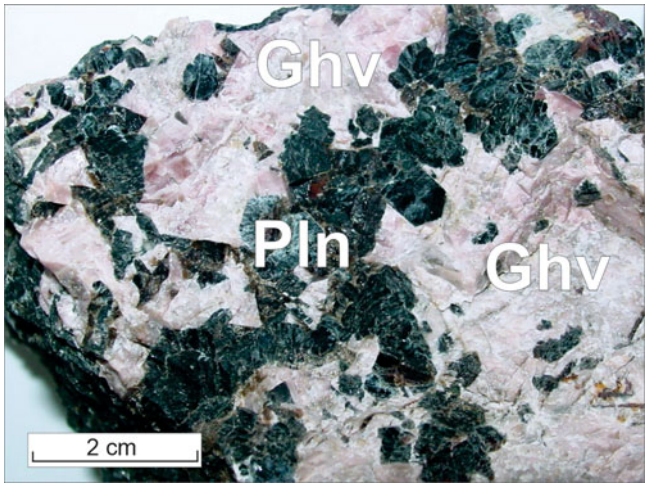

Figure 4. Macroscopic sample of genthelvite from the pegmatite veins hosted by the core albite-enriched granite. Genthelvite (Ghv) occurs surrounding polylithionite (Pln) crystals.

characteristics, genthelvite is considered a mineral of late crystallisation, preceded by the crystallisation of polylithionite and early magmatic quartz and formed before the hydrothermal cryolite.

Genthelvite composition

The helvine-group minerals can be represented by the general formula $A_8^{2+}Be_6Si_6O_{24}S_2$. Structural formulae calculated on the basis of 26 O and S atoms and Be = 6 atoms per formula unit (apfu) (Zito and Hanson, 2017) show cations systematically in deficit on the A site and in excess on the Si site. Therefore, in this study calculations were performed with the following assumptions: the crystal structure is charge balanced; the anion site is fully occupied (i.e. O + S = 26); the Si site is fully occupied by P^{5+}, Si^{4+}, Ti^{4+} and Al^{3+} (preferential order of occupation is P > Si > Ti > Al according to ionic potential); the excess in the Si site (i.e. ^{IV}Si > 6 apfu) is allocated in the ^{IV}Be site with the preferential order of occupation Al > Ti > Si > P with Be^{2+} calculated to yield a total of Be + Si = 12 apfu (i.e. site ^{IV}Be = 6) (Dunn, 1976; Finch, 1990); and the A site has a vacancy (□) and is occupied by U^{4+}, A^{3+} (Ce, Pr, Nd, Sm, Eu, Gd, Ho and Er), A^{2+} (Zn, Fe, Mn, Mg, Pb and Ba) and A^{+} (Na and K) (i.e. site ^{IV}A = 8 − □).

Representative compositions for genthelvite are given in Table 1. The low analytical totals are probably due to the existence of vacancies within the genthelvite structure, hydration as a result of hydrothermal alteration, and the inherent errors associated with Be calculation. The elements P, Ti, Al, REE, Ba, Na and K have concentrations near the detection limits of the EPMA. Consequently, discussions regarding the incorporation of these elements into the crystal structure of genthelvite must be approached with caution. Additionally, low concentrations (hundreds to thousands of ppm) of V, Th, Cr, La, Dy, Tm, Yb, Lu, Bi, Ca, Ni, Sr and Cl were detected. These elements were not considered in the totals of the analyses and in structural calculations.

Genthelvite has a homogeneous composition within individual grains and is characterised as a Mn–Fe-rich genthelvite. It represents a solid solution within the genthelvite–danalite–helvine system, with relatively limited substitutions occurring between Zn^{2+}, Fe^{2+} and Mn^{2+}. However, genthelvite does exhibit moderate overall compositional variability, falling within the range of 36.96 to 49.45 wt.% ZnO, 2.10 to 10.94 wt.% FeO, and 0.61 to 3.03 wt.% MnO. The composition of genthelvite plotted in terms of the relative proportions of Zn, Fe and Mn (expressed as percentages of [Zn + Fe + Mn] atoms) (Fig. 6) reflect the predominance of compositions along the upper part of the Zn–Fe join, although invariably the presence of a small component of helvine occurs.

In genthelvite, other cations that occupy the structural site of Zn, in addition to Mn and Fe, are uncommon, and trace concentrations of K, Ca and Mg are the most commonly reported. In genthelvite from Pitinga the maximum values were 0.062 wt.% MgO, 0.061 wt.% PbO, 0.14 wt.% BaO, 0.33 wt.% Na_2O and 0.05 wt.% K_2O. Uranium concentrations have not been reported in genthelvite from other localities, but in Pitinga it occurs in all genthelvite samples with 0.13 to 0.25 wt.% UO_2. Additionally, the genthelvite samples have high contents of REE (maximum 0.40 wt.% REE_2O_3) relative to that from Cheyenne Canyon (USA, 4.1 ppm REE_2O_3; Zito and Hanson, 2017) and other helvine-group minerals such as the Mn–Zn-rich danalite from Sucuri (Brazil, maximum 363 ppm REE_2O_3; Raimbault and Bilal, 1993) and the Zn–Fe-rich helvine from Dajishan (China, maximum 13 ppm REE_2O_3; Raimbault and Bilal, 1993). The average concentration of light rare earth elements (LREE) (723 ppm) is slightly higher than that of HREE (565 ppm) in genthelvite from Pitinga.

Genthelvite from this work exhibits a REE normalised distribution pattern (Fig. 7) that closely resembles that of the host pegmatite, except for a positive anomaly in Pr and Eu, and the absence of La, Tb, Dy, Tm, Yb and Lu. The mineral incorporated LREE preferentially, although helvine-group minerals have high affinity with HREE (Raimbault and Bilal, 1993; Deer *et al.*, 2004).

The strong negative correlation ($R^2 = 0.963$) between Zn and the sum of the cations Fe, Mn, Mg, Pb, Ba, Na, K, U and REE attest to their location at the A site (Fig. 8a). The positive correlation of Mn and Fe ($R^2 = 0.672$, Fig. 8b) is evidence of their concomitant entrance when substituting for Zn. Concerning the elements in the ^{IV}Be and ^{IV}Si structural sites, the values are similar in all the samples, with little variations in the concentrations of Si (29.30 to 32.19 wt.% SiO_2), S (5.07 to 5.52 wt.% S), and calculated Be (11.73 to 12.49 wt.% BeO). The BeO concentration is similar to those found by inductively coupled plasma atomic emission spectroscopy (ICP–AES) analyses in danalite, which had an average content of 13.1% BeO (Raimbault and Bilal, 1993). In addition, maximum values of 0.38 wt.% P_2O_5, 0.30 wt.% TiO_2 and 0.25 wt.% Al_2O_3 were observed. In contrast to all other minerals found in the pegmatites, genthelvite does not contain fluorine. This absence is probably due to the fact that F has an ionic radius that is too small for sodalite-type structures. The ΣA site gave a negative correlation with Si + Al + P + Ti ($R^2 = 0.900$, Fig. 8c), meaning that the Si substituting for Be is charge balanced by the presence of vacancies at the A site.

Lattice parameters of genthelvite

Genthelvite from the pegmatites associated with the albite-enriched granite have an average *a* parameter of 8.127 Å, varying between 8.117 Å and 8.134 Å (error of 0.00017 Å), which is in accordance with the expected values for this mineral (Table 2). In the helvine-group minerals the constancy of the structural dimensions of the BeO_4 and SiO_4 tetrahedra (Hassan and Grundy, 1985) imply that variations in the unit cell parameter are related to the Mn–Zn–Fe proportions (Oftedal and Saebø, 1963),

https://doi.org/10.1180/mgm.2023.87 Published online by Cambridge University Press

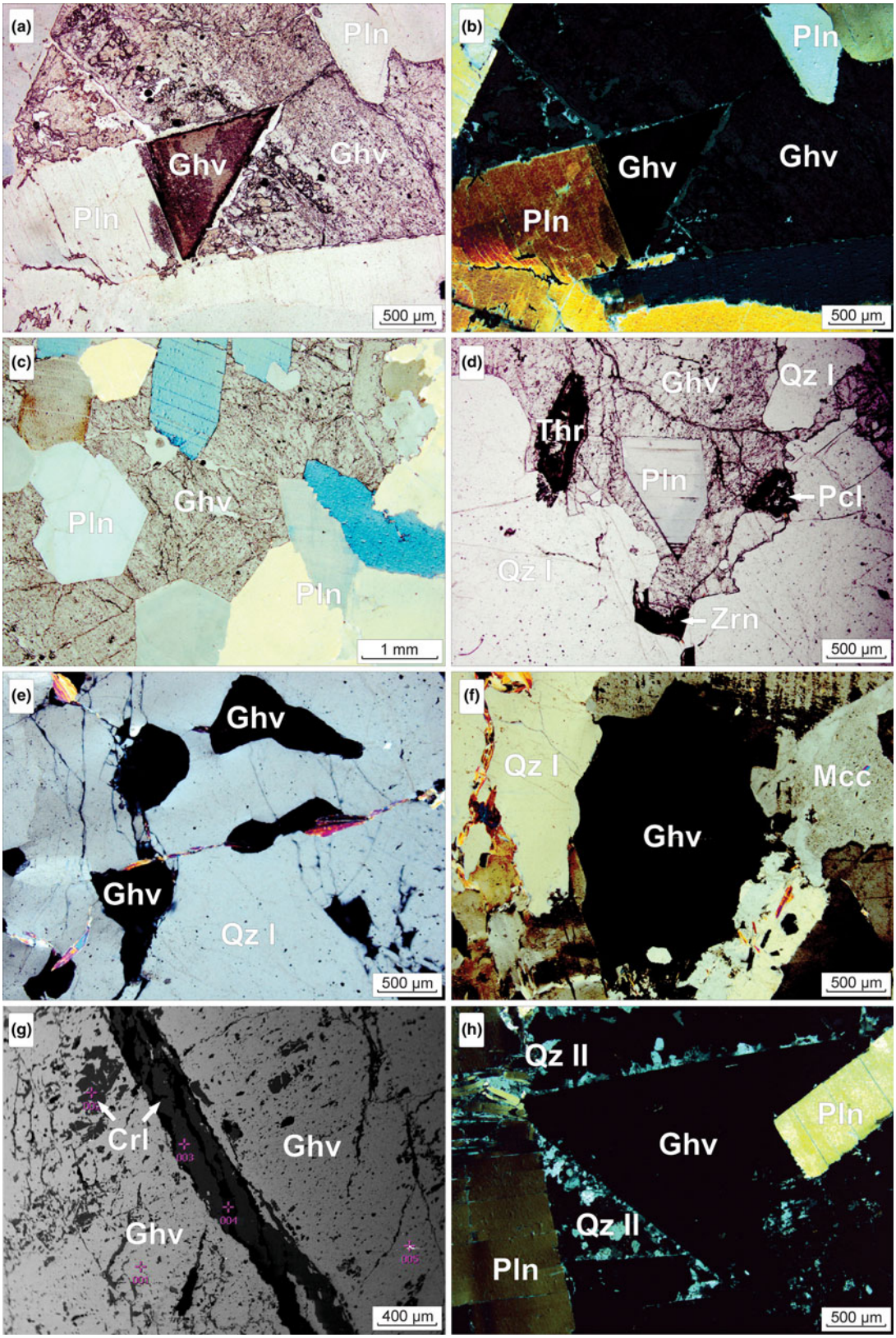

Figure 5. Microphotographs and BSE image of genthelvite from the pegmatite veins hosted by the core albite-enriched granite: (a) typical genthelvite from the pegmatites, with triangular cleavage, associated with polylithionite, plane polarised light (PPL); (b) same as in (a), crossed polarised light (XPL); (c) genthelvite filling the space between polylithionite crystals, PPL; (d) genthelvite associated with magmatic quartz, pyrochlore, thorite and zircon, PPL; (e) genthelvite filling voids in magmatic quartz, XPL; (f) genthelvite in the matrix with magmatic quartz and microcline, XPL; (g) BSE image of genthelvite with microfractures filled by hydrothermal cryolite; (h) hydrothermal quartz along genthelvite growth lines, XPL. Abbreviations: Crl II = hydrothermal cryolite, Ghv = genthelvite, Mcc = microcline, Pcl = pyrochlore, Pln = polylithionite, Qz I = magmatic quartz, Qz II = hydrothermal quartz, Thr = thorite and Zrn = zircon. Mineral symbols after Warr (2021).

https://doi.org/10.1180/mgm.2023.87 Published online by Cambridge University Press

Table 1. Representative compositions from EPMA (wt.%) for Mn–Fe-rich genthelvite in the pegmatite veins hosted by the albite-enriched granite.

Sample	P09.B.2	P09.C.1	P09.C.2	P09.D.15	P09.D.20	P09.D.24	P14.2.4	P14.3.1	P14.3.2	P26.1.3	P26.1.4	P26.1.8	P26.1.9
P_2O_5	0.14	0.38	0.11	n.d.	n.d.	n.d.	0.09	0.26	0.37	n.d.	n.d.	n.d.	n.d.
SiO_2	29.30	29.52	29.79	30.39	32.19	31.27	30.17	30.30	30.27	31.55	31.37	31.55	31.07
UO_2	0.13	0.21	0.23	0.13	0.13	0.14	0.25	0.17	0.22	0.18	0.16	0.14	0.17
TiO_2	n.d.	0.30	0.15	0.13	n.d.	n.d.	0.18	n.d.	n.d.	0.07	n.d.	n.d.	n.d.
Al_2O_3	n.d.	n.d.	0.03	0.04	n.d.	n.d.	0.16	n.d.	n.d.	0.03	n.d.	n.d.	0.25
Ce_2O_3	n.d.	n.d.	n.d.	n.d.	0.11	n.d.	n.d.	n.d.	n.d.	0.08	0.05	n.d.	0.05
Nd_2O_3	n.d.	n.d.	n.d.	0.06	n.d.	n.d.	n.d.	n.d.	0.05	0.03	0.03	n.d.	n.d.
Sm_2O_3	n.d.	n.d.	n.d.	n.d.	n.d.	n.d.	n.d.	0.11	n.d.	n.d.	0.11	n.d.	n.d.
Eu_2O_3	n.d.	n.d.	0.05	0.04	0.07	n.d.	n.d.	0.08	n.d.	n.d.	n.d.	n.d.	0.08
Gd_2O_3	n.d.	n.d.	0.05	n.d.	n.d.	n.d.	n.d.	n.d.	n.d.	n.d.	n.d.	n.d.	n.d.
Ho_2O_3	n.d.	n.d.	0.08	n.d.	n.d.	0.17	n.d.	n.d.	n.d.	n.d.	n.d.	n.d.	n.d.
Er_2O_3	n.d.	n.d.	n.d.	n.d.	0.05	0.04	0.08	n.d.	n.d.	n.d.	0.10	0.04	n.d.
ZnO	44.00	41.41	43.18	41.70	36.96	44.90	49.45	40.56	40.22	46.95	45.76	45.44	45.02
FeO	6.37	08.18	7.66	7.60	10.94	6.03	2.10	9.02	8.95	4.41	4.50	4.84	3.71
MnO	1.13	02.08	1.80	2.64	3.03	1.63	0.61	1.63	2.11	1.52	1.43	1.72	1.75
MgO	0.05	0.02	n.d.	0.02	n.d.	0.02	n.d.	n.d.	n.d.	n.d.	n.d.	n.d.	0.06
PbO	0.03	0.04	n.d.	n.d.	n.d.	n.d.	n.d.	n.d.	n.d.	n.d.	0.04	0.03	0.03
BaO	0.02	0.03	n.d.	0.08	0.06	0.13	0.05	n.d.	n.d.	n.d.	n.d.	0.14	n.d.
BeO*	12.17	12.31	12.49	12.40	12.08	12.41	12.06	12.16	12.19	12.31	12.05	12.11	11.73
Na_2O	n.d.	n.d.	n.d.	0.32	0.03	0.20	n.d.	n.d.	n.d.	0.03	n.d.	n.d.	0.26
K_2O	0.03	n.d.	n.d.	0.02	n.d.	n.d.	0.05	n.d.	n.d.	n.d.	n.d.	0.02	n.d.
S	5.30	5.36	5.52	5.07	5.26	5.33	5.33	5.49	5.51	5.43	5.34	5.43	5.28
$S = O_2$	−2.64	−2.67	−2.75	−2.53	−2.63	−2.66	−2.66	−2.74	−2.75	−2.71	−2.67	−2.71	−2.63
Total	96.01	97.16	98.37	98.12	98.28	99.60	97.92	97.04	97.13	99.87	98.29	98.74	96.83
Structural formulae based on 26 O + S and a sum of 12 apfu in the $^{[IV]}$Be and $^{[IV]}$Si sites													
U^{4+}	0.006	0.010	0.010	0.006	0.006	0.006	0.011	0.008	0.010	0.008	0.007	0.006	0.008
Ce^{3+}	n.d.	n.d.	n.d.	n.d.	0.008	n.d.	n.d.	n.d.	n.d.	0.005	0.004	n.d.	0.003
Nd^{3+}	n.d.	n.d.	n.d.	0.004	n.d.	n.d.	n.d.	n.d.	0.004	0.002	0.002	n.d.	n.d.
Sm^{3+}	n.d.	n.d.	n.d.	n.d.	n.d.	n.d.	n.d.	0.008	n.d.	n.d.	0.008	n.d.	n.d.
Eu^{3+}	n.d.	n.d.	0.003	0.003	0.005	n.d.	n.d.	0.005	n.d.	n.d.	n.d.	n.d.	0.005
Gd^{3+}	n.d.	n.d.	0.003	n.d.	n.d.	n.d.	n.d.	n.d.	n.d.	n.d.	n.d.	n.d.	n.d.
Ho^{3+}	n.d.	n.d.	0.005	n.d.	n.d.	0.010	n.d.	n.d.	n.d.	n.d.	n.d.	n.d.	n.d.
Er^{3+}	n.d.	n.d.	n.d.	n.d.	0.003	0.002	0.005	n.d.	n.d.	n.d.	0.006	0.002	n.d.
Zn^{2+}	6.642	6.143	6.367	6.122	5.348	6.511	7.347	6.010	5.942	6.793	6.722	6.638	6.686
Fe^{2+}	1.089	1.374	1.280	1.265	1.793	0.991	0.354	1.514	1.497	0.723	0.749	0.801	0.624
Mn^{2+}	0.196	0.353	0.304	0.445	0.503	0.271	0.105	0.278	0.358	0.252	0.241	0.288	0.299
Mg^{2+}	0.015	0.006	n.d.	0.007	n.d.	0.005	n.d.	n.d.	n.d.	n.d.	n.d.	n.d.	0.019
Pb^{2+}	0.002	0.002	n.d.	n.d.	n.d.	n.d.	n.d.	n.d.	n.d.	n.d.	0.002	0.001	0.001
Ba^{2+}	0.002	0.002	n.d.	0.006	0.005	0.010	0.004	n.d.	n.d.	n.d.	n.d.	0.011	n.d.
Na^{+}	n.d.	n.d.	n.d.	0.123	0.011	0.075	n.d.	n.d.	n.d.	0.013	n.d.	n.d.	0.103
K^{+}	0.008	n.d.	n.d.	0.006	n.d.	n.d.	0.012	n.d.	n.d.	n.d.	n.d.	0.004	n.d.
$\Sigma_{[IV]A}$	7.959	7.891	7.972	7.986	7.682	7.882	7.838	7.822	7.810	7.797	7.742	7.752	7.748
Be^{2+}	5.977	5.942	5.995	5.925	5.689	5.857	5.831	5.864	5.862	5.797	5.759	5.758	5.668
Al^{3+}	n.d.	n.d.	0.005	0.012	n.d.	n.d.	0.051	n.d.	n.d.	0.008	n.d.	n.d.	0.081
Ti^{4+}	n.d.	0.045	n.d.	0.020	n.d.	n.d.	0.027	n.d.	n.d.	0.010	n.d.	n.d.	n.d.
Si^{4+}	0.023	0.013	n.d.	0.043	0.311	0.143	0.091	0.136	0.138	0.185	0.241	0.242	0.251
$\Sigma_{[IV]Be}$	6.000	6.000	6.000	6.000	6.000	6.000	6.000	6.000	6.000	6.000	6.000	6.000	6.000
P^{5+}	0.032	0.082	0.023	n.d.	n.d.	n.d.	0.020	0.056	0.081	n.d.	n.d.	n.d.	n.d.
Si^{4+}	5.968	5.918	5.950	6.000	6.000	6.000	5.980	5.944	5.919	6.000	6.000	6.000	6.000
Ti^{4+}	n.d.	n.d.	0.022	n.d.	n.d.	n.d.	n.d.	n.d.	n.d.	n.d.	n.d.	n.d.	n.d.
Al^{3+}	n.d.	n.d.	0.005	n.d.	n.d.	n.d.	n.d.	n.d.	n.d.	n.d.	n.d.	n.d.	n.d.
$\Sigma_{[IV]Si}$	6.000	6.000	6.000	6.000	6.000	6.000	6.000	6.000	6.000	6.000	6.000	6.000	6.000
O^{2-}	23.969	23.982	23.934	24.112	24.067	24.040	23.990	23.935	23.934	24.004	24.008	23.987	24.011
S^{2-}	2.031	2.018	2.066	1.888	1.933	1.960	2.010	2.065	2.066	1.996	1.992	2.013	1.989
Σ_X	26.000	26.000	26.000	26.000	26.000	26.000	26.000	26.000	26.000	26.000	26.000	26.000	26.000

*BeO calculated considering a total of Be + Si = 12 apfu; n.d. = not detected.

as well as the proportions of other elements in the A site. For genthelvite from Pitinga and other localities (Table 2), the correlation between the average *a* parameter and the average Mn content is strongly positive ($R^2 = 0.84$, Fig. 9a), but with the average Zn + Fe content this parameter presents a strong negative trend ($R^2 = 0.89$, Fig. 9b). Though there is a moderate overlap of unit cells, as indicated by the error bars, the correlation can be associated tentatively with the ionic radii of the elements. The ionic radius is larger for Mn (0.66 Å) and smaller for Zn (0.60 Å) and Fe (0.63 Å) (Shannon, 1976).

Discussion

Geological environment of genthelvite occurrences

Beryllium is a rare element both in meteorites and on Earth, but it is a crustal element par excellence, with an average of 2.1 ppm BeO in rocks of the upper continental crust, in contrast to 1.4 ppm BeO in the lower crust and 0.07 ppm BeO in the mantle (Rudnick and Gao, 2005). The first paragenesis of magmas are formed by minerals whose structure inhibits the capture of Be in melting. Therefore, Be enrichment occurs in the final stages

https://doi.org/10.1180/mgm.2023.87 Published online by Cambridge University Press

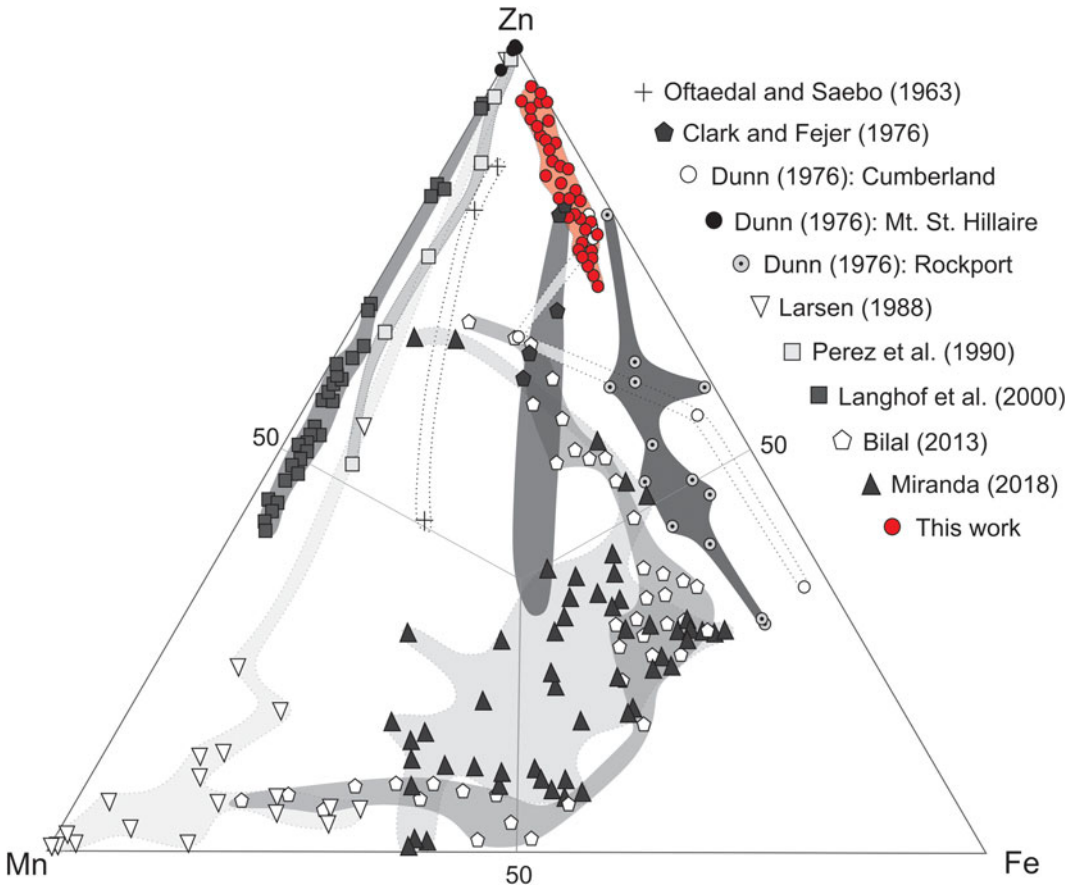

Figure 6. Compositions of genthelvite, danalite and helvine expressed as percentages of Zn + Fe + Mn atoms.

of magmatic crystallisation, mainly in granitic pegmatites and alkaline rocks (Grew, 2002). In the later stages of differentiation, there is a supersaturation of SiO_2 and accumulation of alkalis and volatiles, allowing the formation of Be minerals and quartz (Pulz *et al.*, 1998).

A significant majority of occurrences of genthelvite are in pegmatites and in late-formation rocks as hydrothermal veins, greisens and skarns, associated with alkaline to peralkaline granites and syenites (Table 3). These occurrences have in common a highly evolved magma enriched in high-field-strength elements and associated hydrothermal events and/or metasomatism. The genthelvite investigated occurs in pegmatite veins that represent the most evolved fluid of a peralkaline magmatic system, but contrast with other genthelvite occurrences of the world showing an unusual mineralogical association and geochemical trend.

Mineral assemblages of genthelvite worldwide

Considering the stability fields of minerals, genthelvite can be formed from willemite and phenakite; willemite can be altered to sphalerite; genthelvite can be altered to sphalerite and phenakite or bertrandite; and all of them together with quartz (Burt, 1988). Therefore, commonly associated minerals with genthelvite are quartz, feldspar, micas and other Zn-bearing phases such as sphalerite, willemite and gahnite, as well as other Be-containing phases such as phenakite and bertrandite (Burt, 1988). There is also willemite in these associations, especially in peralkaline rocks. Genthelvite with willemite, phenakite, Na-fluorides as gagarinite, weberite and pachnolite have been reported in metasomatic peralkaline rocks from Russia (Kudrin, 1978). In the Ilimaussaq Complex, Greenland, willemite with chkalovite was reported as the only Be-bearing mineral, whereas genthelvite was found at a different location within the Complex (Metcalf-Johnson, 1977). In Mont St. Hilaire, Canada, willemite and genthelvite were reported, together with sphalerite and galena (Bank, 1975; Dunn, 1976).

In this investigation, genthelvite is the only Be-bearing phase, and it is associated with polylithionite, riebeckite, quartz, microcline, albite, xenotime, cryolite and the accessory phases pyrochlore, columbite, zircon, gagarinite, galena, sphalerite and hematite. Beryl, willemite and phenakite or bertrandite were not observed. This occurrence is notably unusual because it lacks the helvine-group minerals danalite and helvine, which are commonly associated with genthelvite in other deposits. This absence is probably linked to the physical-chemical conditions discussed below. In peralkaline conditions, genthelvite associated with aluminous minerals such as beryl and topaz are restricted, but genthelvite with Na-fluorides are typical (Burt, 1988), as observed in the genthelvite–cryolite association in the Pitinga pegmatites.

Controls on genthelvite composition

Crystallographic and structural data, the ionic radius of the A-site cations and the structural geometric model, indicate that complete miscibility should exist between the three end-members of the helvine–genthelvite–danalite solid solution (Hassan and

https://doi.org/10.1180/mgm.2023.87 Published online by Cambridge University Press

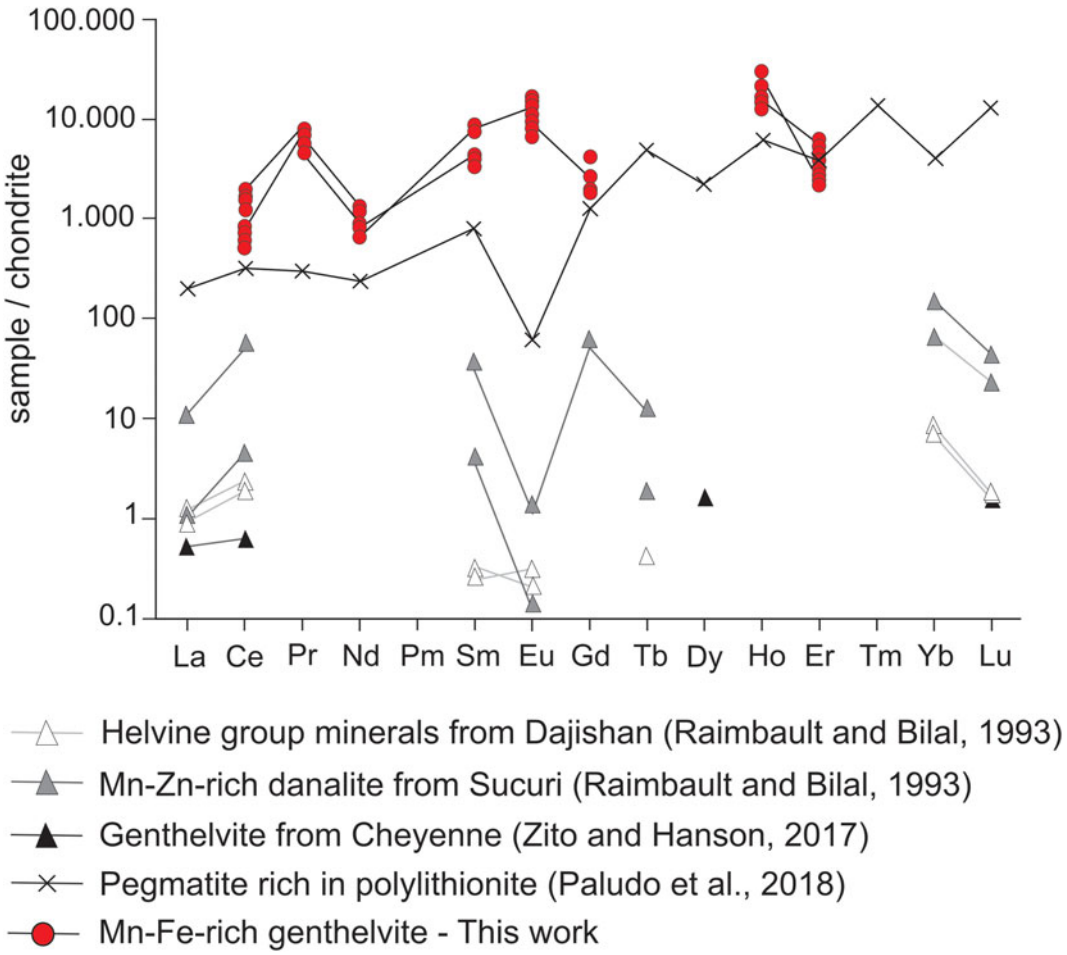

Figure 7. Chondrite-normalised REE patterns (chondrite of Anders and Grevesse, 1989).

Grundy, 1985), however, there are apparent compositional gaps in the Zn–Fe, Zn–Mn and Mn–Fe trends, and pure danalite has not been observed in Nature (Oftedal and Saebø, 1963; Clark and Fejer, 1976; Dunn, 1976; Larsen, 1988; Perez *et al.*, 1990; Langhof *et al.*, 2000; Bilal, 2013). According to Antao and Hassan (2010) the absence of pure danalite in Nature might simply indicate that another phase is more stable than danalite.

Genthelvite in this investigation has high concentrations of Zn and small concentrations of Fe in comparison with genthelvite from the Rockport Deposit, Massachusetts, USA (Dunn, 1976) and from the Cairngorm Mountains, UK (Clark and Fejer, 1976). It also has a higher Zn and lower Fe and Mn content than the more Mn–Fe-enriched genthelvite reported from Cumberland, Rhode Island, USA (Dunn, 1976) and from the Sucuri Granite in Brazil (Miranda, 2018). It is also different from the typical Fe–Mn-rich genthelvite reported in Norway (Oftedal and Saebø, 1963; Larsen, 1988), the Air Mountains of Niger (Perez *et al.*, 1990) and Uto, Sweden (Langhof *et al.*, 2000). Finally, with this work we demonstrate the existence of natural genthelvite in the upper Zn–Fe trend of the Zn–Fe–Mn ternary diagram (Fig. 6), filling a compositional gap.

Genthelvite is one of only two known silicates in which Zn and Be occur together. Regardless that Zn (ionic radius 0.60 Å; Shannon, 1976) and the much smaller Be (ionic radius 0.27 Å; Shannon, 1976) represent different chemical affinities, they both have the tendency to be concentrated by fractionated crystallisation and to adopt four-fold coordination (Burt, 1988). Iron and Mn (^{IV}Mn = 0.66 Å, ^{IV}Fe = 0.63 Å; Shannon, 1976) also adopt this coordination. Regardless of these coordination controls compositional variations in helvine-group minerals have been shown to have a direct association with temperature and S and O fugacity, rather than with the availability of Zn, Fe and Mn in the fluid. An investigation of several genthelvite crystals from a granitic massif (Antao and Hassan, 2010) showed that Mn-rich genthelvite formed at lower temperatures than Mn-poor genthelvite. In the Taghouaji Alkaline Complex, Niger, Mn-poor genthelvite occurs with sphalerite and galena in a low f_{O_2} and high f_{S_2} environment and a crystallisation temperature higher than 375°C, whereas the Mn-rich genthelvite occurs with hematite at temperatures of ~288°C (Perez *et al.*, 1990).

The Mn-poor composition of the genthelvite investigated here is probably influenced by its formation at relatively high temperatures, in a low f_{O_2} and high f_{S_2} environment. However, the significant variation in Zn–Fe content between individual grains (36.96 to 49.45 wt.% ZnO, 2.10 to 10.94 wt.% FeO) is probably controlled by the local mineral assemblage. In the magmatic stage of the pegmatite veins, Fe and Zn were buffered by the presence of riebeckite (~30 wt.% FeO + Fe_2O_3; ~2 wt.% ZnO) and polylithionite (~6 wt.% FeO; ~1 wt.% ZnO). In these minerals, the Mn content is typically <1 wt.% MnO (Paludo *et al.*, 2018). Additionally, the available Pb and S combined to form magmatic galena. During the early hydrothermal

https://doi.org/10.1180/mgm.2023.87 Published online by Cambridge University Press

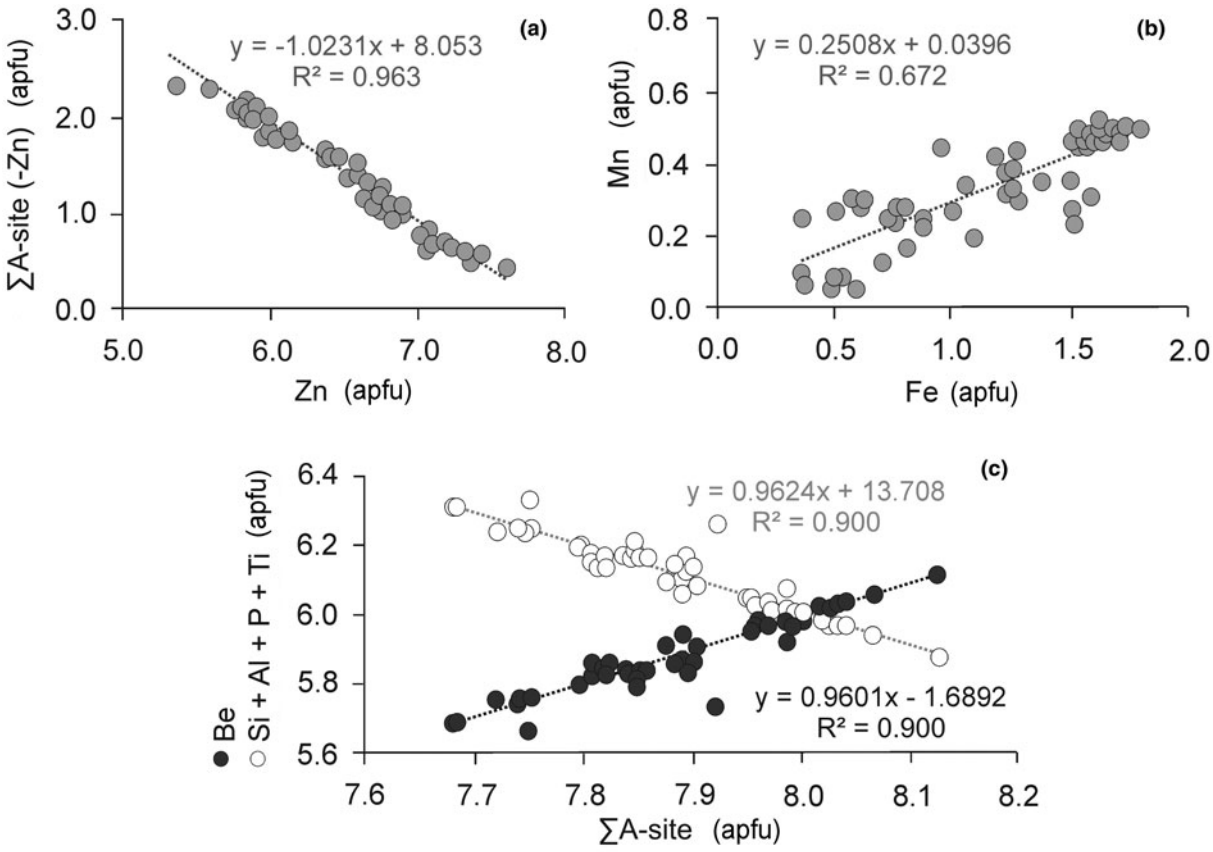

Figure 8. Binary diagrams for genthelvite from the pegmatites associated with the albite-enriched granite: (a) ΣA site (– Zn) versus Zn; (b) Mn versus Fe; and (c) ΣA site versus Be and ΣA site versus Si + Al + P + Ti. Concentrations are expressed in apfu.

Table 2. Crystallographic parameters of genthelvite from the pegmatites (Madeira deposit, Pitinga Mine) and other localities, in descending order of the average of parameter *a*.

Locality	↓ *a* (Å)	*a* (error)	Average wt. %			Reference
			Zn	Fe	Mn	
Air Mountains, Nigeria	8.165	n.a.	39.61	1.31	10.52	Perez *et al.* (1990)
Kymi, Finland	8.140	±0.01	44.79	2.47	6.55	Haapala and Ojanperã (1972)
Cairngorms, Scotland	8.139	n.a.	42.60	7.30	2.80	Clark and Fejer (1976)
Cairngorms, Scotland	8.133	±0.005	37.00	9.90	5.80	Morgan (1967)
Pitinga, Brazil	8.127	±0.00017	43.5	6.49	1.78	This work
Jos, Nigeria	8.120	±0.01	40.56	11.73	1.72	Von Knorring and Dyson (1959)
Mt. St. Hilaire, Canada	8.119	n.a.	52.20	0.01	0.12	Antao and Hassan (2010)

Abbreviations: n.a. = not available.

stage, Fe was incorporated into altered thorite and altered pyrochlore, whereas both Fe and Mn were widely incorporated into secondary Mn–Fe-rich columbite. Zinc and S were incorporated into secondary sphalerite, and the remaining available S formed galena and pyrite. In the late hydrothermal stage, Fe contributed to the formation of hematite, surrounding all the previous formed minerals (Minuzzi *et al.*, 2005; Bastos Neto *et al.*, 2009; Hadlich *et al.*, 2019). Genthelvite crystallised during the transition between the magmatic and hydrothermal stages of pegmatite evolution, following the crystallisation of riebeckite and polylithionite. Thus, the compositional variation in the genthelvite is closely related to the prior formation of these minerals, which played a significant role in buffering the Fe content relative to Zn in their immediate vicinity.

These variations in composition are also verified by the REE contents. Genthelvite from Pitinga has a REE pattern enriched in LREE relative to its host pegmatite. The average LREE content is slightly higher than that of HREE content, which differs from those of other localities, which have higher HREE contents. The HREE enrichment in relation to the LREE in the helvine-group minerals from Sucuri, Brazil and Dajishan, China (Raimbault and Bilal, 1993) was attributed by these authors only to crystallographic controls. The higher concentration of HREE in danalite from Cheyenne, USA (Zito and Hanson, 2017), was

https://doi.org/10.1180/mgm.2023.87 Published online by Cambridge University Press

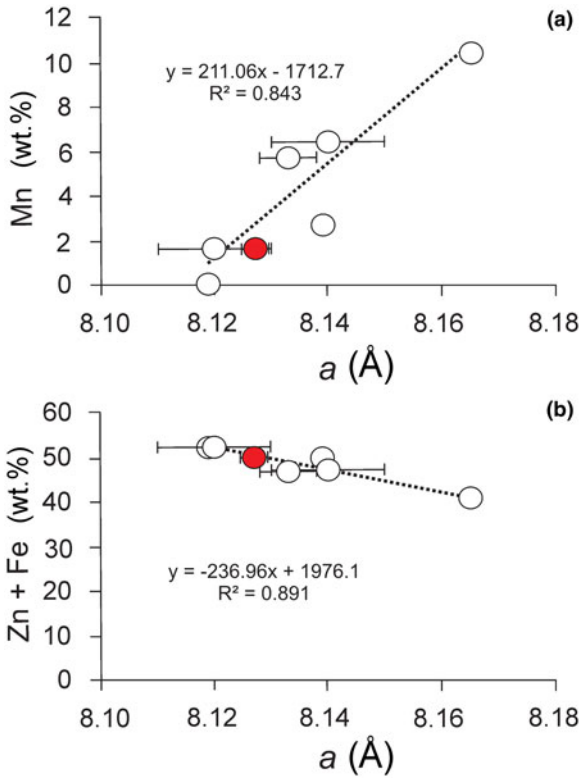

Figure 9. Correlation of the unit cell parameter *a* (Å) versus the Mn (a) and Zn + Fe (b) concentrations of genthelvite from Pitinga (this work, filled circle) and other localities (open circles, Table 2). Mn, Zn and Fe are expressed as wt.%. The bars indicate the error for the parameter *a*.

attributed to the presence of late F-enriched fluids. At Pitinga, the REE are primarily concentrated in xenotime (with a predominance of HREE as Dy, Yb and Lu, Bastos Neto *et al.*, 2012) and polylithionite. As these minerals crystallise before genthelvite, the REE content in genthelvite is lower and skewed towards the LREE, even though the late-stage fluids are rich in fluorine. The Eu positive anomaly probably reflects a reducing magma in which the Eu^{2+} could preferentially substitute for Zn^{2+} and because of the crystallisation of albite instead of anorthite in the pegmatites.

The possibility that the presence of REE and U in genthelvite might result from hydrothermal alteration cannot be ruled out. In such a scenario, the incorporated U might have originated from the alteration of U–Pb–LREE-bearing pyrochlore into columbite during the early hydrothermal stage of the pegmatite veins (Hadlich *et al.*, unpublished work). The released Pb was incorporated predominantly into secondary galena, whereas the U found partial accommodation within secondary U-rich columbite, and solid solutions of thorite–coffinite–xenotime and zircon.

Origin of genthelvite

Few Be-bearing minerals form in the magmatic stage of pegmatite consolidation, with beryl being dominant (Černý, 2002). Paragenetically late (supercritical-to-hydrothermal) beryllium minerals are divided in two broad categories: (1) alteration products of the early phases of Be; (2) minerals occuring in miarolitic cavities and fissures (Černý, 2002). In the pegmatites investigated, genthelvite is observed as massive aggregates of crystals surrounding pegmatitic crystals and including accessory minerals. This observation can be interpreted as the crystallisation of a late-evolved fluid, wherein Be was preserved though complexation (e.g. with F) as no other Be mineral is present.

Compositional zoning or intergrowths between helvine-group minerals is relatively common (Haapala and Ojanperä, 1972; Clark and Fejer, 1976; Perez *et al.*, 1990; Antao and Hassan, 2010), and is attributed to changes in the physical-chemical conditions during crystallisation, such as temperature and S fugacity. The preservation of this zoning or intergrowths would require low-temperature crystallisation and a rapid crystallisation process (Antao and Hassan, 2010). On the basis of these observations, it is plausible to infer that the lack of zoning in the genthelvite grains signifies diffusion between Zn, Fe and Mn. This diffusion process is probably facilitated by a relatively slow crystallisation within the late-evolved fluids of pegmatite formation, which occurred under relatively high temperatures.

The mineralogical and petrographic variations of the albite-enriched granite were mapped and described in detail in Bastos Neto *et al.* (2009), and the fluid-inclusion assemblies or associations in Ronchi *et al.* (2011). In these investigations, it was concluded that the large hydrothermal massive cryolite deposit in the centre of albite-enriched granite is part of an evolutionary process of a magma originally rich in volatiles, which during its polyphase crystallisation process resulted in the exsolution of hydrothermal saline deuteric fluids (salinity between 0 and 25% eq. NaCl and homogenisation temperatures from 100 to 400° C). Furthermore, the authors concluded that these fluids lowered the solidus of the system, within the albite-enriched granite dykes of the pegmatitic albite-enriched granite and pegmatite veins. In this process, phases rich in microcline, polylithionite, cryolite and genthelvite were formed and hydrothermal alteration was promoted, resultiing in albitisation, silicification, clay-formation, fluoritisation and oxidation of iron-rich minerals.

In the pegmatite veins, hosted by the albite-enriched granite, the sequence of genthelvite formation following riebeckite and polylithionite suggests that genthelvite is one of the last minerals to crystallise. However, it does form prior to hydrothermal cryolite, which is observed corroding genthelvite crystals. This observation emphasises the strong association of genthelvite with the transitional period between the late magmatic and early hydrothermal stages of pegmatite evolution.

Genthelvite formation conditions

Genthelvite is a rare mineral compared to other Be-bearing minerals or even to other members of the helvine group, as a result of its small stability field (Burt, 1988). The elements that constitute genthelvite (Zn, Mn, Fe, Be, Si and S) are commonly found as trace elements in highly fractionated granitic systems, therefore, this mineral is typical of systems at a late stage of differentiation, in which stability is due to local and transient conditions, generally atypical in the consolidation of granitic pegmatites, including low alumina activity and relatively reducing conditions that facilitate the coexistence of sulfides and silicates (Burt, 1988; Bilal and Fonteilles, 1988).

Genthelvite stability in a paragenesis is restricted to systems with low S activity (Burt, 1988). Because of the differing chalcophile behaviour of Zn>>Fe>Mn, in systems with high SO_{-1} (the acid anhydride of H_2S), the Zn_2SiO_4 component would have been destabilised to form an assemblage with sphalerite and quartz (Burt, 1988). In contrast, under low SO_{-1}

https://doi.org/10.1180/mgm.2023.87 Published online by Cambridge University Press

Table 3. The genthelvite investigated from Madeira deposit, Pitinga Mine, Brazil and comparison with other occurrences.

Geological environment	Location	Host rock	Mineral paragenesis (secondary)		Refs.
			Major	Accessory	
Granitic rocks and Greisens	Madeira Granite, Pitinga, Brazil	Pegmatite veins in albite-enriched granite	Quartz, albite, microcline, riebeckite, polylithionite, cryolite, xenotime (hydrothermal quartz and cryolite)	zircon, thorite, pyrochlore, columbite, cassiterite, gagarinite, galena, sphalerite, hematite	(1)
	El Paso County, Colorado, USA	Pegmatite cavity in Pikes Peak granite	Quartz, microcline, albite, mica, (sericite), fluorite	Danalite, Fe-columbite, ilmenite, Ce-bastnäsite, (goethite)	(2), (3)
	Utö, Sweden	Granitic LCT-type Pegmatite	Albite, K-feldspar	Sphalerite, helvine, milarite, chiavennite	(4)
	Keivy Alkaline Province, Russia	Pegmatite in peralkaline granite	Quartz, amazonite, albite, biotite, muscovite	Beryl, garnet, covellite, gadolinite	(5)
	Younger Granite, Jos-Bukuru, Nigeria	Albite vein in biotite-enriched granite	Albite, Li-mica	Thorite, columbite inclusions, zircon, cassiterite	(6)
		Pegmatite in biotite-enriched granite	Microcline, amazonite, Li-mica		(6)
	Sucuri Granite, Goiás, Brazil	Hydrothermal albitite associated with biotite granite	Albite	Biotite, fluorite, danalite, allanite, chalcopyrite, sphalerite, pyrite, pyrrhotite, galena, cubanite	(7), (9), (8)
	Rhode Island, USA	Granite	Quartz	Fluorite, aegirine, zircon	(10)
	Eurajoki Massive, Finland	Greisen in rapakivi granite	Quartz, (sericite), (chlorite)	Topaz, sphalerite, cassiterite, galena, chalcopyrite, fluorite, (Fe–Ti oxides)	(11)
	Granitic Complex, Kymi, Finland	Greisen in biotite-enriched rapakivi granite	Muscovite phengite, (chlorite), ± quartz, ± relict feldspar	Fluorite, ± apatite, ± cassiterite, monazite, zircon, (Fe–Ti oxides, chalcocite, malachite)	(11), (12)
	Mangabeira Granite, Goiás, Brazil	Greisen associated with topaz-albite-enriched granite	Quartz, Li-mica	Topaz, helvine	(13), (14)
Alkaline rocks	Rovgora, Kola Peninsula, Russia	Pegmatite associated with alkaline granite	Amazonite, quartz, biotite	Ilmenite, fluorite, pyrochlore	(15)
	Cairngorm Mountains, Scotland	Pegmatite cavity in quartz monzonite (adamellite)	Quartz, microcline, oligoclase	Chlorite, bertrandite, (kaolin)	(16), (17)
	Lovozero, Russia	Nepheline syenite pegmatite	Feldspar, sodalite	Mn-ilmenite, zircon, apatite	(18)
	Oslo region, Norway	Nepheline syenite pegmatite	Analcime, mica	Zircon, bastnäsite, natrolite, pyrophanite, eudidymite	(19)
		Nepheline syenite pegmatite	Analcime, albite, muscovite	Sphalerite, galena, aegirine, catapleiite, astrophyllite, pyrophanite, monazite, fluorite	(19)
	Stokkøy, Langesundsfjord, Norway	Nepheline syenite pegmatite associated with monzonite	Nepheline, microcline, acmite, biotite, albite	Helvine, magnetite, zircon, melanite, titanite, pyrochlore, apatite, fluorite, analcime, meliphanite, sulfides	(20)
	Bratthagen, Lågendalen, Norway	Syenite pegmatite associated with monzonite	Microcline	Catapleiite, pyrochlore, analcime	(20)
	Ilimaussaq, Greenland	Albite vein in alkaline intrusion	Albite, aegirine	Neptunite, catapleiite	(21)
	Bolshaya Turupya, Mankhambovsky, Urals, Russia	Alkaline metassomatite associated with granitoid	Quartz	Columbite, pyrochlore, bastnäsite, allanite, zircon, euclase, phenacite, fluorite	(22)
Calc-silicate rocks and skarns	Treburland, Cornwall, England	Calc-silicate rock associated with granite	Calcite, garnet, chlorite, diopside	Wollastonite, idocrase, axinite, galena, molybdenite, pyrite, pyrrhotite, arsenopyrite	(23)*
	Pitkäranta, Karella, Russia	Calc-silicate rock near rapakivi granite	Fluorite, biotite, chlorite	Vesuvianite	(24)
	Sterling Hill, Ogdensburg, New Jersey, USA	Rhodonite skarn and augite skarn	Rhodonite, augite, actinolite, quartz, calcite, albite	Willemite, galena, scheelite, barite, titanite, zircon, sphalerite	(25), (26)

References: (1) This work; (2) Glass *et al*. (1944); (3) Zito and Hanson (2017); (4) Langhof *et al*. (2000); (5) Vasil'ev (1961); (6) Von Knorring and Dyson (1959); (7) Raimbault and Bilal (1993); (8) Bilal (2013); (9) Miranda (2018); (10) Dunn (1976); (11) Haapala and Ojanperä (1972); (12) Haapala and Lukkari (2005); (13) Botelho (1992); (14) Freitas (2000); (15) Lunts and Saldau (1963); (16) Morgan (1967); (17) Clark and Fejer (1976); (18) Es'kova (1957); (19) Oftedal and Saebø (1963); (20) Larsen (1988); (21) Bollinberg and Petersen (1967); (22) Dushin *et al*. (2018); (23) Kingsbury (1961); (24) Bulakh and Frank-Kamenetsky (1961); (25) Cianciulli and Verbeek (2003); (26) Leavens *et al*. (2009)
*Findings by Kingsbury are considered dubious see e.g. Ryback *et al*. (1998)

conditions danalite and helvine are not stable, and the instability of the FeS and MnS components will lead to the formation of silicates or oxides (Burt, 1988). The low content of Fe in genthelvite also indicates high O_2 fugacity during crystallisation, with the crystallisation of hematite (Burt, 1980).

The wide compositional variation in helvine-group minerals, genthelvite in the core and danalite in the border, in the albitites associated with the Sucuri Granite (Brazil) suggest that the increased alkalinity (albitisation) in the system favoured genthelvite growth and the subsequent increase in S fugacity favoured

https://doi.org/10.1180/mgm.2023.87 Published online by Cambridge University Press

danalite crystallisation by the reaction: $Zn_8Be_6Si_6O_{24}S_2 + 8FeS_2 \leftrightarrow Fe_8Be_6Si_6O_{24}S_2 + 8ZnS + 4S_2$ (Miranda, 2018).

Within the albite-enriched granite, the pegmatites originated through a process of continuous magma fractionation, resulting in a peralkaline composition highly enriched in high-field-strength elements. The extensive crystallisation of microcline, albite and polylithionite effectively buffered the Al content in the later fluids, reducing the alumina activity within the system. Simultaneously, the late-stage magmatic processes involved in the genesis of the pegmatites were characterised by a substantial increase in fluorine content (Paludo *et al.*, 2018). The pegmatites that are rich in amphibole have ~3.35 wt.% F, whereas the ones rich in polylithionite have ~4.80 wt.% F, and those rich in cryolite have an average of 37.32 wt.% F. The remarkably high concentration of fluorine, coupled with the crystallisation of magmatic galena, effectively lowered the fugacity of H_2S, thus stabilising genthelvite during the transition from the late magmatic to the early hydrothermal stages of pegmatite evolution. The low Fe content in genthelvite can be attributed to the prior incorporation of Fe into riebeckite and polylithionite and indicates an O activity that is too elevated to favour danalite formation. The widespread formation of Mn and Fe oxides (columbite and hematite) during the hydrothermal stage further underscores the high O activity within the system.

Conclusion

This investigation of genthelvite in pegmatite veins hosted by the Madeira albite-enriched granite has yielded the following conclusions.

Among the various pegmatites hosted by the albite-enriched granite, the genthelvite-bearing bodies are rich in riebeckite, polylithionite and xenotime, confirming the observations by Paludo *et al.* (2018).

Genthelvite was formed during the transition between the late magmatic and early hydrothermal stages of pegmatite evolution. It stands out as the sole Be-bearing mineral in this context. Its formation can be attributed to Be being preserved in the late-evolved fluid, probably by complexation with fluorine. Genthelvite crystallised surrounding polylithionite, riebeckite, quartz, xenotime, pyrochlore, thorite and zircon, and it was subsequently corroded by hydrothermal cryolite.

Genthelvite exhibits a homogeneous composition within individual grains, but the overall composition displays moderate variation. It is characterised as a Mn–Fe-rich genthelvite, forming a solid solution within the genthelvite–danalite–helvine system. The mineral features relatively high levels of Zn (36.96 to 49.45 wt.% ZnO), lower Mn content (0.61 to 3.03 wt.% MnO), and variable Fe content (2.10 to 10.94 wt.% FeO), in comparison to the compositions found in other locations, and fills a compositional gap along the upper part of the Zn–Fe join in the Zn–Fe–Mn ternary diagram. Genthelvite exhibits elevated U levels (up to 0.25 wt.% UO_2), and significant REE contents (up to 0.40 wt.% REE_2O_3). Notably, the average LREE content is higher than that of HREE, a deviation from compositions found in other locations, where HREE content tends to be the higher one. Additionally, genthelvite from this site lacks fluorine. Regardless of these compositional disparities, the crystallographic parameters ($a = 8.127$ Å) of genthelvite from the pegmatite veins closely resemble those determined for crystals from other localities.

The unusual composition of genthelvite is attributed to the buffering of Fe, F and HREE by minerals that crystallised before genthelvite. These include riebeckite, polylithionite, xenotime and magmatic cryolite.

Genthelvite was affected during the late hydrothermal stage, which was associated with F-rich aqueous fluids responsible for the formation of the massive cryolite deposit, and the disseminated hydrothermal cryolite within the albite-enriched granite. The highest observed fluid-inclusion homogenisation temperature of 400°C, measured in hydrothermal cryolite (Bastos Neto *et al.*, 2009), establishes the minimum initial temperature for the hydrothermal process. The structure of genthelvite facilitated the incorporation of Fe, Mn, Mg, Pb, Ba, Na, K, U and REE into the Zn^{2+} structural site. Additionally, it allowed the allocation of excess Si, Al, Ti and P to the ^{IV}Si and ^{IV}Be structural sites. The high levels of U and REE substituting for Zn, as well as Si substituting for Be, are charge balanced by the presence of vacancies at the A site.

This crystallochemical study of genthelvite has revealed that its formation occurred in an alkaline and subaluminous environment, under stable conditions within the late-evolved fluids, and at relatively high temperatures (>400°C), in a reducing environment. The substantial presence of fluorine and the crystallisation of magmatic galena effectively reduced the fugacity of H_2S, ensuring the stability of genthelvite during the transition from the late magmatic to early hydrothermal stages in the evolution of the albite-enriched granite. The moderate variation in Fe content within genthelvite can be attributed primarily to the presence of riebeckite and polylithionite, which acted as buffers for Fe content in their immediate surroundings. In addition, the extensive formation of Mn and Fe oxides (columbite and hematite) during the hydrothermal stage, underscores an O activity that is too high to favour the formation of danalite.

Acknowledgements. This work was supported by Conselho Nacional de Desenvolvimento Científico e Tecnológico (CNPq) through the Project 405839/2013-2018 and for granting scholarship. The authors thank the reviewers and editors for their contributions to improving the manuscript.

Supplementary material. The supplementary material for this article can be found at https://doi.org/10.1180/mgm.2023.87.

Competing interests. The authors declare none.

References

Almeida F.F.M., Hasui Y., Brito Neves B.B. and Fuck R.A. (1981) Brazilian structural Provinces: an introduction. *Earth Sciences Reviews*, **17**, 1–29.

Anders E. and Grevesse N. (1989) Abundances of the elements: Meteoritic and solar. *Geochimica et Cosmochimica Acta*, **53**, 197–214.

Antao S.M. and Hassan I. (2010) A two-phase intergrowth in genthelvite from Moint Saint-Hilaire, Quebec. *The Canadian Mineralogist*, **48**, 1217–1223.

Bank H. (1975) Durchsichtiger schleifwuerdiger blauer Willemit vom Mt. St. Hilaire in Kanada. *Zeitschrift der Deutsche Gemnologische Gesellschaft*, **24**, 250–256.

Bastos Neto A.C., Pereira V.P., Ronchi L.H., Lima E.F. and Frantz J.C. (2009) The worldclass Sn, Nb, Ta, F (T, REE, Li) deposit and the massive cryolite associated with the albite-enriched facies of the Madeira A-type granite, Pitinga Mining District, Amazonas State, Brazil. *The Canadian Mineralogist*, **47**, 1329–1357.

Bastos Neto A.C., Pereira V.P., Pires A.C., Barbanson L. and Chauvet A. (2012) Fluorine-rich xenotime from the Nb-Ta-Sn Madeira world-class deposit associated with the albite-enriched granite at Pitinga, Amazonia, Brazil. *The Canadian Mineralogist*, **50**, 1019–1032.

Bastos Neto A.C., Ferron T.M.M., Chauvet A., Chemale F., Lima E.F., Barbanson L. and Costa C.F.M. (2014) U-Pb dating of the Madeira Suite and structural control of the albite-enriched granite at Pitinga (Amazônia, Brazil): evolution of the A-type magmatism and implications

for the genesis of the Madeira Sn-Ta-Nb (REE, cryolite) world-class deposit. *Precambrian Research*, **243**, 181–196.

Bilal E. (2013) Geochimie et conditions de cristallisation des mineraux du groupe de l'helvite, *Geonomos*, **2**, 1–13.

Bilal E. and Fonteilles M. (1988) Conditions d'apparition respectives de l'helvite, de la phénacite et du béryl dans l'environnement granitique: exemple du massif de Sucuri (Brésil). *Comptes Rendus de l'Académie des Sciences*, **307**, 273–276.

Bollinberg H. and Petersen O.V. (1967) Genthelvite from the Ilimaussaq alkaline intrusion, south Greenland. *Medelelser om Gronland*, **181**(4), 1–9.

Botelho N.F. (1992) *Les ensembles granitiques subalcalins a peralumineux mineralisés em Sn et In de la sous-province Paraná, état de Goiás, Brésil*. PhD dissertation, Université de Paris VI, France.

Bulakh A.G. and Frank-Kamenetsky V.A. (1961) *Geological excursion in the vicinity of Pitkyaranta* Publishing house of the KASSR, Petrozavodsk, 108 pp. [in Russian].

Burt D.M. (1980) The stability of danalite $Fe_4Be_3(SiO_4)S$. *American Mineralogist*, **65**, 355–360.

Burt D.M. (1988) Stability of genthelvite, $Zn_4(BeSiO_4)_3S$: an exercise in chalcophilicity using exchange operators. *American Mineralogist*, **73**, 1384–1394.

Černý P. (2002) Mineralogy of beryllium in granitic pegmatites. Pp. 405–444 in: *Beryllium: Mineralogy, petrology, and geochemistry*, Vol. 50 (E.S. Grew, editor). Reviews in Mineralogy and Geochemistry, Mineralogical Society of America, Virginia.

Černý P. and Ercit T.S. (2005) The classification of granitic pegmatites revisited. *The Canadian Mineralogist*, **43**, 2005–2026.

Cianciulli J.C. and Verbeek E.R. (2003) Genthelvite from Ogdensburg, New Jersey. *The Picking Table*, **44**(2), 23–26.

Clark A.M. and Fejer E.E. (1976) Zoned genthelvite from the Cairngorm Mountains, Scotland. *Mineralogical Magazine*, **40**, 637–639.

Costi H.T. (2000) *Petrologia de granitos alcalinos com alto flúor mineralizados em metais raros: o exemplo do Albita-granito da Mina Pitinga, Amazonas, Brasil*. PhD dissertation, Universidade Federal do Pará, Brazil.

Costi H.T., Dall'agnoll R. and Moura C.A.V. (2000) Geology and Pb-Pb Geochronology of Paleoproterozoic volcanic and granitic rocks of Pitinga province, Amazonian craton, northern Brazil. *International Geology Review*, **42**, 832–849.

Costi H.T., Borges R.M. and Dall'agnoll R. (2005) Depósitos de estanho da mina Pitinga, estado do Amazonas. Pp. 391-475 in: *Caracterização de depósitos minerais em distritos mineiros da Amazônia* (O.J. Marini, E.T. Queiroz and B.W. Ramos, editors). DNPM-CT/MINERAL-ADIMB, Brasília.

Costi H.T., Dall'Agnol R., Pichavant M. and Ramo O.T. (2009) The peralkaline tin-mineralized Madeira cryolite albite-rich granite of Pitinga, Amazonian craton, Brazil: petrography, mineralogy and crystallization processes. *The Canadian Mineralogist*, **47**, 1301–1327.

Deer W.A., Howie R.A., Wise W.S. and Zussman J. (2004) *The Rock-forming Minerals Series: framework silicates (silica minerals, feldspathoids and the zeolites)*. The Geological Society, London, 988 pp.

Dill H.G. (2016) The CMS classification scheme (Chemical composition-Mineral assemblage-Structural geology)-linking geology to mineralogy of pegmatitic and aplitic rocks. *Journal of Mineralogy and Geochemistry*, **193**, 231–263.

Dolejs D. and Baker D.R. (2007) Liquidus equilibria in the system K_2O-Na_2O-Al_2O_3-SiO_2-F_2O to 100 MPa 2: differentiation paths of fluorosilicic magmas in hydrous systems. *Journal of Petrology*, **48**, 807–828.

Dunn P.J. (1976) Genthelvite and the helvine group. *Mineralogical Magazine*, **40**, 627–636.

Dushin V.A., Prokopchuk D.I., Koz'min V.S., Zhuklin E.A. and Trutnev A.K. (2018) Geology and mineral resources of the Mankhambovsky Block (subpolar Urals). *News of the Ural State Mining University*, **3**, 19–33.

Es'kova E.M. (1957) Genthelvite from alkaline pegmatites. *Doklady Akademii Nauk*. 153, 681–683 [in Russian].

Ferron J.M.T.M., Bastos Neto A.C., Lima E.F., Costi H.T., Moura C.A.V., Prado M. and Galarza M.A. (2006) Geologia e cronologia Pb-Pb de rochas graníticas e vulcânicas ácidas a intermediárias paleoproterozóicas da Província de Pitinga, Cráton Amazônico. *Revista Brasileira de Geociências*, **36**, 499–512.

Finch A.A. (1990) Genthelvite and willemite, zinc minerals associated with alkaline magmatism from the Motzfeldt centre, south Greenland. *Mineralogical Magazine*, **54**, 407–412.

Freitas M.E. (2000) *A evolução dos greisens e mineralização estanífera no Morro do Laranjinha – Maciço Granítico Mangabeira – Goiás*. PhD dissertation, Universidade de Brasília, Brazil.

Glass J.J., Jahns R.H. and Stevens R.H. (1944) Helvite and danalite from New Mexico and the helvite group. *American Mineralogist*, **29**, 163–191.

Grew E.S. (2002) Mineralogy, petrology and geochemistry of beryllium: An introduction and list of beryllium minerals. Pp. 487–549 in: *Beryllium: Mineralogy, Petrology, and Geochemistry* (E.S. Grew, editor). Reviews in Mineralogy and Geochemistry, Vol. 50. Mineralogical Society of America, Virginia, USA.

Haapala I. and Lukkari S. (2005) Petrological and geochemical Evolution of the Kymi stock, a topaz granite cupola within the Wiborg rapakivi batholith, Finland. *Lithos*, **80**, 347–362.

Haapala I. and Ojanperä P. (1972) Genthelvite-Bearing Greisens in southern Finland. *Geological Survey of Finland Bulletin*, **259**.

Hadlich I.W., Bastos Neto A.C., Botelho N.F. and Pereira V.P. (2019) The thorite mineralization in the Madeira Sn-Nb-Ta world-class deposit (Pitinga, Brazil), *Ore Geology Reviews*, **105**, 445-466.

Hassan I. and Grundy H.D. (1985) The crystal structure of helvite group minerals, $(Mn, Fe, Zn)_8(Be_6Si_6O_{24})S_2$. *American Mineralogist*, **70**, 186–192.

Holland T.J.B. and Redfern S.A.T. (1997) Unit cell refinement from powder diffraction data: the use of regression diagnostics. *Mineralogical Magazine*, **61**, 65–77.

Horbe M.A., Horbe A.C., Costi H.T. and Teixeira J.T. (1991) Geochemical characteristics of cryolite-tin-bearing granites from the Pitinga mine, northwestern Brazil – a review, *Journal of Geochemical Exploration*, **40**, 227-249.

Kingsbury A.W.G. (1961) Beryllium minerals in Cornwall and Devon: helvine, genthelvite, and danalite. *Mineralogical Magazine*, **32**, 921–940.

Kudrin V.S. (1978) Rare metal alkaline quartz-albite-microcline metasomatites (qualmites) of zones of regional metamorphism (in Russian). Pp. 183–194 in: *Metasomatism and ore deposition* (D.S. Korzhinskii, editor). Nauka Press, Moscow.

Langhof J., Holtstam D. and Gustafsson L. (2000) Chiavennite and zoned genthelvite-helvite as late-stage minerals of the Proterozoic LCT pegmatites at Utö, Stockholm, Sweden. *GFF*, **122**, 207–212.

Larsen A.O. (1988) Helvite group minerals from syenite pegmatites in the Oslo Region, Norway. *Norsk Geologisk Tidsskrift*, Report, 68.

Leavens P.B., Zullo J. and Verbeek E. (2009) A complex, genthelvite-bearing skarn from the Passaic pit, Sterling Hill mine, Ogdensburg, New Jersey. *Axis*, **5**, 1–26.

Lengler H.F. (2016) *Pegmatitos do albita granito Madeira: avaliação do minério para fins de beneficiamento*. Monographe, Universidade Federal do Rio Grande do Sul, Brazil.

Lenharo S.L.R. (1998) *Evolução magmática e modelo metalogenético dos granitos mineralizados da região de Pitinga, Amazonas, Brasil*. PhD dissertation, Universidade de São Paulo, Brazil.

Lenharo S.L.R., Pollard P.J. and Born H. (2003) Petrology and textural evolution of granites associated with tin and rare-metals mineralization at the Pitinga mine, Amazonas, Brazil, *Lithos*, **66**, 37-61.

Lunts A.J. and Saldau E.P. (1963) Genthelvite from pegmatites on the Kola peninsula (in Russian). *Zapiski Vserossiyskogo Mineralogicheskogo Obshchestva*, **92**, 81–84.

Martin R.F. (2006) A-type granites of crustal origin ultimately result from open-system fenitization-type reactions in an extensional environmental. *Lithos*, **91**, 125–136.

Metcalf-Johnson J. (1977) Willemite from the Ilimaussaq alkaline intrusion. *Mineralogical Magazine*, **41**, 71–75.

Minuzzi O.R.R. (2005) *Gênese e evolução da mineralização de criolita, pirocloro e columbita da subfacies albita granito de núcleo, Mina Pitinga, Amazonas, Brasil*. PhD dissertation, Universidade Federal do Rio Grande do Sul, Brazil.

Minuzzi O.R.R., Bastos Neto A.C., Pereira V.P. and Flores J.A.A. (2006) The massive cryolite deposit and the disseminated ore of cryolite from the Pitinga mine (Amazon, Brazil). *Revista Brasileira de Geociências*, **36**, 104–123.

https://doi.org/10.1180/mgm.2023.87 Published online by Cambridge University Press

Miranda A.C.R. (2018) *Caracterização da mineralização de estanho e índio do maciço Sucuri, província estanífera de Goiás*. Master dissertation, Universidade de Brasília, Brazil.

Morgan W.C. (1967) Genthelvite and bertrandite from the Cairngorm Mountains, Scotland. *Mineralocal Magazine*, **36**, 60–63.

Oftedal I. and Saebø P.C. (1963) Classification of some Norwegian members of the helvine group. *Norsk Geologisk Tidsskrift*, **43**, 405–409.

Paludo C.M., Bastos Neto A.C., Pereira V.P. and Botelho N.F. (2018) Mineralogia e geoquímica de pegmatitos ricos em ETR, F e metais alcalinos associados à fácies albita granito no depósito de Sn-Nb-Ta-(F, ETR, U, Th) Madeira (mina Pitinga, AM, Brasil). *Pesquisas em Geociências*, **45**, 1–28.

Perez J.-P., Dusausov Y., Babkine J. and Pagel M. (1990) Mn zonation and fluid inclusions in genthelvite from the Taghouaji complex (Aïr Mountains, Niger). *American Mineralogist*, **75**, 909–914.

Pierosan R., Lima E.F., Nardi L.V.S., Bastos Neto A.C., Campos C.P., Jarvis K., Ferron J.M.T.M. and Prado M. (2011) Geochemistry of Paleoproterozoic volcanic rocks of the Iricoume Group, Pitinga Mining District, Amazonian craton, Brazil. *International Geology Review*, **53**, 946–976.

Pulz G.M., Cunha M.C.L. and Formoso M.L.L. (1998) Revisão sobre a geoquímica do berílio nos materiais naturais. *Pesquisas*, **25**, 29–40.

Raimbault L. and Bilal E. (1993) Trace-element contents of helvite-group minerals from metasomatic albitites and hydrothermal veins at Sucuri, Brazil and Dajishan, China. *The Canadian Mineralogist*, **31**, 119–127.

Ronchi F.C., Althoff F.J., Bastos Neto A.C. and Dill H.G. (2019) Structural control of REE-pegmatites associated with the world-class Sn-Nb-Ta-cryolite deposit at the Pitinga mine, Amazonas, Brazil. *Pesquisas em Geociências*, **46**, 1–14.

Ronchi L.H., Bastos Neto A.C., Gedoz S.C., Weber M.L., Pereira V.P. and Andrek M. (2011) A transição magmático-hidrotermal registrada por inclusões fluidas no albita-granito de núcleo, Mina Pitinga, Amazonas. Pp. 71–88 in: *Contribuições à metalogenia do Brasil*, (J.C. Frantz, J.M. Charão and H. Jost, editors). Serviço Geológico do Brasil, Porto Alegre, Brazil.

Rudnick R.L. and Gao S. (2005) Composition of the continental crust. Pp. 1–61 in: *The Crust*, Vol. 3 (R.L. Rudnick, editor). Treatise on Geochemistry, Elsevier-Pergamon, Oxford.

Ryback G., Clark A.M. and Stanley C.J. (1998) Re-examination of the A.W.G. Kingsbury Collection of British Minerals at the Natural History Museum, London. *Geological Curator*, **6**, 317–322.

Santos J.O.S., Hartmann L.A., Gaudete H.E., Groves D.I., McNaughton N.J. and Fletcher L.R.A. (2000) New understanding of the Provinces of Amazon Craton based on Integration of Field Mapping and U-Pb and Sm-Nd geochronology. *Gondwana Research*, **3**, 453–488.

Shannon R.D. (1976) Revised effective ionic radii and systematic studies of interatomic distances in halides and chalcogenides. *Acta Crystallographica*, **A32**, 751–767.

Simões M.S.S., Almeida M.E., Souza A.G.H., Silva B.D.P.B. and Rocha P.G. (2014) Characterization of the volcanic and hypabyssal rocks of the Paleoproterozoic Iricoumé Group in the Pitinga region and Balbina Lake area, Amazonian craton, Brazil: petrographic distinguishing features and emplacement conditions. *Journal of Volcanology and Geothermal Research*, **286**, 138–147.

Stolnik D. (2015) *Caracterização da xenotima na fácies pegmatítica do albita granito de núcleo, Pitinga (AM)*. Monography, Universidade Federal do Rio Grande do Sul, Brazil.

Vasil'ev V.A. (1961) On genthelvite. *Zapiski Vsesoyuznogo Mineralogicheskogo Obshchestva*, **90**, 571–578 [in Russian].

Veiga Jr. J.P., Nunes A.C.B., Fernandes A.S., Amaral J.E., Pessoa M.R. and Cruz S.A.S. (1979) *Projeto Sulfetos de Uatumã*. Departamento Nacional de Pesquisa Mineral/Serviço Geológico do Brasil, Relatório Final, 7.

Von Knorring O. and Dyson P. (1959) An occurrence of genthelvite in the Younger Granite Province of northern Nigeria. *American Mineralogist*, **44**, 1294–1298.

Warr L.N. (2021) IMA-CNMNC approved mineral symbols. *Mineralogical Magazine*, **85**, 291–320.

Zito G. and Hanson S.L. (2017) Genthelvite overgrowths on danalite cores from a pegmatite miarolitic cavity in Cheyenne Canyon, El Paso County, Colorado. *The Canadian Mineralogist*, **55**, 195–206.

https://doi.org/10.1180/mgm.2023.87 Published online by Cambridge University Press